The Meteoritical Society

Meteoritics & Planetary Science 48, Nr 7, 1296–1324 (2013)
doi: 10.1111/maps.12047

Testing the ureilite projectile hypothesis for the El'gygytgyn impact: Determination of siderophile element abundances and Os isotope ratios in ICDP drill core samples and melt rocks

S. GODERIS[1,2*], A. WITTMANN[3,4], J. ZAISS[5], M. ELBURG[6,7], G. RAVIZZA[5], F. VANHAECKE[2], A. DEUTSCH[8], and P. CLAEYS[1]

[1]Department of Geology, Earth System Science, Vrije Universiteit Brussel, Pleinlaan 2, Brussels BE-1050, Belgium
[2]Department of Analytical Chemistry, Ghent University, Krijgslaan 281-S12, Ghent BE-9000, Belgium
[3]Department of Earth and Planetary Sciences, Washington University St. Louis, Campus Box 1169, 1 Brookings Dr., St. Louis, Missouri 63130–4899, USA
[4]Lunar and Planetary Institute, 3600 Bay Area Blvd., Houston, Texas 77058 USA
[5]Department of Geology and Geophysics, University of Hawaii at Manoa, Honolulu, Hawai'i USA
[6]Department of Geology & Soil Sciences, Ghent University, Krijgslaan 281-S8, Ghent BE-9000, Belgium
[7]School of Agricultural, Earth and Environmental Sciences, University of KwaZulu-Natal, Durban, South Africa
[8]Institut für Planetologie, Westfälische Wilhelms-Universität Münster, Wilhelm-Klemm-Str. 10, Münster D-48149, Germany
*Corresponding author. E-mail: Steven.Goderis@vub.ac.be

(Received 15 February 2012; revision accepted 29 October 2012)

Abstract–The geochemical nature of the impactites from International Continental Scientific Drilling Project—El'gygytgyn lake drill core 1C is compared with that of impact melt rock fragments collected near the western rim of the structure and literature data. Concentrations of major and trace elements, with special focus on siderophile metals Cr, Co, Ni, and the platinum group elements, and isotope ratios of osmium (Os), were determined to test the hypothesis of an ureilite impactor at El'gygytgyn. Least squares mixing calculations suggest that the upper volcanic succession of rhyolites, dacites, and andesites were the main contributors to the polymict impact breccias. Additions of 2–13.5 vol% of basaltic inclusions recovered from drill core intervals between 391.6 and 423.0 mblf can almost entirely account for the compositional differences observed for the bottom of a reworked fallout deposit at 318.9 mblf, a polymict impact breccia at 471.4 mblf, and three impact melt rock fragments. However, the measured Os isotope ratios and slightly elevated PGE content (up to 0.262 ng g^{-1} Ir) of certain impactite samples, for which the CI-normalized logarithmic PGE signature displays a relatively flat (i.e., chondritic) pattern, can only be explained by the incorporation of a small meteoritic contribution. This component is also required to explain the exceptionally high siderophile element contents and corresponding Ni/Cr, Ni/Co, and Cr/Co ratios of impact glass spherules and spherule fragments that were recovered from the reworked fallout deposits and from terrace outcrops of the Enmyvaam River approximately 10 km southeast of the crater center. Mixing calculations support the presence of approximately 0.05 wt% and 0.50–18 wt% of ordinary chondrite (possibly type-LL) in several impactites and in the glassy spherules, respectively. The heterogeneous distribution of the meteoritic component provides clues for emplacement mechanisms of the various impactite units.

INTRODUCTION

The El'gygytgyn Impact Crater

El'gygytgyn is an 18 km diameter, 3.58 ± 0.04 Ma old, very well preserved impact crater centered at 67°30′ N and 172°34′ E on the NE Siberian Chukotka peninsula (Gurov et al. 1978; Layer 2000; Gurov and Koeberl 2004). An asymmetrically offset, 12 km diameter and up to 170 m deep lake, which is studied for its paleoclimatic record (e.g., Nowaczyk et al. 2002; Melles et al. 2005, 2011, 2012; Gebhardt et al. 2006), occupies the central depression. El'gygytgyn's central crater contains a 7–7.5 km diameter and 2 km wide central ring, instead of a central uplift. Seismic data document the stratigraphic succession in the central crater (Gebhardt et al. 2006) with a 170 m thick upper and a 190–250 m thick lower lacustrine sedimentary unit underlain by 100–400 m thick impact breccias lying on top of fractured bedrock.

A generalized preimpact upper target stratigraphy of 83.2–89.3 Ma old volcanic rocks (Belyi 1998; Layer 2000; Gurov et al. 2007) was established by Gurov and Gurova (1991) and comprises, from top to bottom, 250 m rhyolitic ignimbrites, 200 m of rhyolitic tuffs and lavas, 70 m of andesitic tuffs and lavas, and 100 m of rhyolitic and dacitic ash tuffs and welded tuffs. Paleocene basalts intruded this target assemblage (e.g., Glushkova and Smirnov 2005). Gurov et al. (1978, 1979, 2005), Gurov and Koeberl (2004), Feldman et al. (1981), Dabizha and Feldman (1982), and Kapustina et al. (1985) carried out petrographic work on shock metamorphosed rocks that occur on lake terraces and glacial deposits around the crater.

Geochemical studies of impactites from El'gygytgyn revealed enrichments in certain siderophile elements (e.g., Cr, Co, Ni, Ir), interpreted to reflect contamination with a meteoritic component. On the basis of resemblance of relative abundances of these siderophile elements in glassy melt bombs from El'gygytgyn to those of ureilites, Va'lter et al. (1982) characterized the impactor as a ureilite. Kapustina et al. (1985) studied volatilization trends of elements, including siderophiles in El'gygytgyn impactites. These authors confirmed the findings of Va'lter et al. (1982). Gurov and Koeberl (2004) presented additional trace element data for glassy impact melt from El'gygytgyn and concluded that an achondrite appears to be the most probable impactor type based on the relatively high Cr enrichment, but cautioned that "… no unambiguous conclusions regarding the presence and nature of a meteoritic component in the El'gygytgyn impactites can be made so far."

From February 2009 until May 2009, the Austrian Federal Ministry of Science and Research; the Federal Ministry of Education and Research, Germany; the International Continental Scientific Drilling Project (ICDP) Germany—German Science Foundation; the Russian Academy of Sciences; and the U.S. National Science Foundation funded the drilling of three holes ("Site 5011-1") on the frozen crater lake of El'gygytgyn. The deepest hole 1C, near the center of the lake penetrated 225.3 m of lacustrine sediments and 207.5 m of impactites, of which only 157.4 m (76%) were recovered, to a final depth of 517.3 m below the lake floor (mblf; Melles et al. 2011; Koeberl et al. 2013).

Impactor Identification

So far, distinct projectiles have been proposed (e.g., Tagle and Hecht 2006; Koeberl 2007; Goderis et al. 2012) for less than 20% of the 183 impact structures recognized on Earth today (Earth Impact Database 2012). During crater formation on a solid planetary surface, the impactites incorporate traces of meteoritic material (vapor, melt, or solid fragments) that induce a geochemical signature distinct from local or average crustal values. On Earth, in addition to atypical isotope ratios (e.g., $^{187}Os/^{188}Os$, $^{53}Cr/^{52}Cr$, and $^{54}Cr/^{52}Cr$), elevated concentrations of specific siderophile elements (e.g., Cr, Co, Ni, and the platinum group elements [PGEs: Ru, Rh, Pd, Os, Ir, Pt]) and inter-element ratios (e.g., Rh/Ir, Pt/Pd, etc.) can be used to constrain the extraterrestrial components of impactites. Because PGE concentrations in chondrites (Tagle and Berlin 2008) are generally two to four orders of magnitude higher than common terrestrial crustal or mantle abundances, these highly siderophile elements are ideally suited for the detection and characterization of minute amounts of extraterrestrial material admixed in impactites. However, this approach is of limited use for PGE-poor meteorites, including specific types of differentiated achondrites. In terrestrial impactites, bulk meteoritic contributions generally amount to less than 1 wt% (Koeberl 2007). Normally, projectile contributions in terrestrial impactites occur in impact melt rock (e.g., Palme et al. 1978, 1981; McDonald et al. 2001; McDonald 2002; Tagle and Claeys 2005). Nonetheless, other impactites can also contain enrichments in projectile components, as documented for the distal ejecta distributed worldwide at the Cretaceous-Paleogene (K/Pg) boundary (e.g., Alvarez et al. 1980; Smit and Hertogen 1980; Claeys et al. 2002). Due to its diluted concentration, meteoritic material is often heterogeneously distributed in impact melt rocks compared with the more uniform composition in major (and some trace) elements (Grieve et al. 1977). For

El'gygytgyn, Va'lter et al. (1982) suggest that impact melt bombs have the highest probability to contain a meteoritic component, based on a comparison with melt bombs from the Zhamanshin impact crater. In the latter, drop-shaped irghizites carry pronounced traces of contamination by meteoritic matter, whereas massive impactites (zhamanshinites) do not (e.g., Palme et al. 1981). Previous studies of the siderophile element content in impact melt rocks and glasses of the El'gygytgyn impact structure have detected only minor enrichments in Cr, Co, Ni, and Ir (on the order of approximately 100 pg g^{-1} Ir; Va'lter et al. 1982; Kapustina et al. 1985; Gurov and Koeberl 2004).

We aimed to geochemically characterize the impactite section in drill core samples of ICDP-El'gygytgyn hole 1C, including comparison with impact melt rock fragments that were collected on the surface of the crater. One goal is the reconstruction of the proportion of target rock components that contributed to the polymict impact breccias. The second goal is the identification of a meteoritic component using siderophile element abundances and Os isotope ratios in the available impactite samples. Finally, we want to characterize the nature and distribution of projectile components throughout the impactite drill core section.

SAMPLES

Seventeen samples were selected from the impactite section of the El'gygytgyn ICDP 1C drill core for geochemical characterization (Table 1). Based on macroscopic (Fig. 1a–f) and thin section examination, the drill core was stratigraphically subdivided (see Wittmann et al. 2012). Its upper part consists of lacustrine deposits that are followed by a reworked fallout deposit from 315.4 to 319.4 mblf. This unit is underlain by suevite (polymict breccia with rare impact melt particles) from 319.4 to 329.1 mblf with core loss masking the boundary toward the top of the upper polymict impact breccia (330.8–419.3 mblf). The lower portion of the drill core consists of monomictly brecciated ignimbrites that contain mafic inclusions between 420.3 to 420.9 mblf and 422.4 to 422.7 mblf, and a section of lower polymict breccia between 471.3 and 472.1 mblf. Major units below the lacustrine deposit were sampled for geochemical characterization (Fig. 2), with a main focus on the reworked fallout deposit, suevite, and polymict impact breccia. In the reworked fallout deposit, glass spherules (Fig. 3), diaplectic quartz glass with coesite, quartz with planar deformation features (PDF), and millimeter-sized impact melt particles occur. The reworked fallout deposit appears to be composed of 7–11 fining-upward sequences of breccias, gravels, and sands topped by lacustrine

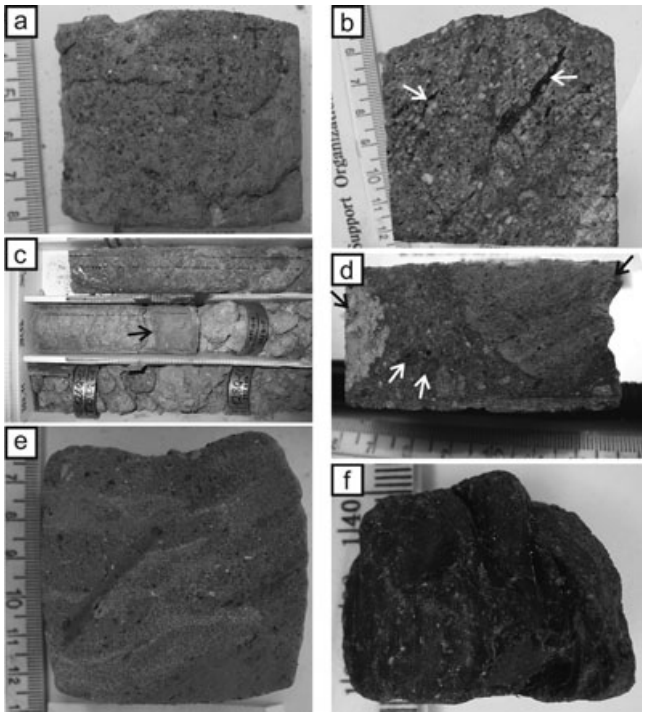

Fig. 1. a) Lower polymict impact breccia sample 471.4 mblf; b) upper ignimbrite sample 435.4 mblf, note dark brown melt streaks (arrows) elongated in a uniform direction; c) green, mafic inclusion sample 391.6 mblf (arrow) in brecciated ignimbrite of core box 126, core diameter is approximately 6.6 cm; d) suevite sample 326.1 mblf with two tuff clasts (black arrows) at left and right end of sample, and two possible mantled clasts (white arrows); e) reworked fallout deposit sample 318.9 mblf, note medium sand matrix that embeds slivers of fine-grained breccia; f) glassy impact melt clast TM17; ruler scales in all sample photographs are in cm.

background sedimentation. Based on spherule-bearing samples 318.9, 317.6, and 316.7 mblf, abundances vary from 0.8 to 1.4 spherules cm^{-2} (Wittmann et al. 2012). Assuming a mean spherule diameter of 0.3 mm, extrapolation of the lower spherule abundance over the thickness of the reworked fallout deposit results in a spherule layer that was originally approximately 10 mm thick (Wittmann et al. 2012). In the underlying suevite, diagnostic shock metamorphic features are rare and mainly present in form of up to 0.4 cm long isotropic, glassy impact melt particles. The underlying polymict breccia and ignimbrite are mostly devoid of diagnostic shock features (Raschke et al. 2013; Wittmann et al. 2012). Consequently, the reworked fallout deposit and suevite units are the units that most likely contain a meteoritic component. It was either directly incorporated during the main phase of crater formation or added as fallback material toward the end of the cratering process.

In addition, three glassy impact melt rock fragments (12–28 g in mass; 2–5 cm long) collected

Table 1. Petrographic descriptions of the El'gygytgyn ICDP drill core samples and impact melt rocks analyzed in this study.

Sample depth (mblf)	Lithology	Microscopic description	Sample mass (g)	Analytical methods
316.7	Reworked fallout deposit	Layered and size-sorted, matrix-supported polymict microbreccia with few shock metamorphic features in quartz and feldspar and few glassy impact melt shards, and three spherules, one of which is hollow. One round hole may be a trace of where a spherule was plucked during preparation of the thin section.	95.14	ICP-OES, NiS-ICP-MS, NiS-ID-ICP-MS
317.6	Reworked fallout deposit	Unsorted polymict breccia with up to 7 mm long felsic volcanic clasts. It contains 3 grains of diaplectic quartz glass with coesite and abundant <<1 mm-size impact melt shards, and a few quartz clasts with PDF. Four glass spherules occur, two of which contain Ni-rich spinel, and one of which is hollow. Also, one spherule-shaped hole is present, where a spherule was plucked.	59.72	ICP-OES, NiS-ICP-MS, NiS-ID-ICP-MS
318.9	Reworked fallout deposit	Up to 1 cm long, polymict microbreccia fragments are embedded in a sand matrix. Exclusively in the breccia domains, one 0.15 mm diameter spherule with Ni-rich spinel grains and 8 round to oval, 0.1 to 0.23 mm diameter holes where spherules were plucked during preparation of the thin section occur. No shock metamorphic features or impact melt particles are present.	54.67	ICP-OES, NiS-ICP-MS, NiS-ID-ICP-MS
323.9	Suevite	The sample is a polymict breccia with variegated clasts of felsic and mafic volcanics, including gray tuff clasts. All clasts appear more strongly affected by hydrothermal alteration than in the other samples of this sub-unit. Few features that may indicate a low (<10 GPa) shock metamorphic overprint occur and the few impact melt particles have a yellowish color, suggesting alteration.	47.86	ICP-OES, NiS-ICP-MS
325.7	Suevite	Just one quartz grain with possible planar fractures occurs, but this sample contains the largest vesicular, glassy impact melt particle in the suevite unit with a length of 3.6 mm along with a few more shard-shaped impact melt particles. Felsic volcanics, mainly tuff and basalt, constitute the bulk of clast material.	26.87	ICP-OES, NiS-ICP-MS
326.1	Suevite	Thin section captures two >1 cm size tuff clasts that sandwich a domain of polymict impact breccia that contains felsic and mafic volcanics and several isotropic, vesicular impact melt particles, typically 0.1 mm in size. A 1 mm shocked quartz clast occurs with 2 sets of intersecting, undecorated PDF.	46.38	ICP-OES, NiS-ICP-MS
327.8	Suevite	Light gray, vesicular (tuff) clast that has a very low density	14.24	ICP-OES, NiS-ICP-MS
328.1	Suevite	Layered polymict breccia with an upper part that is clast-supported and a lower, porous domain that is matrix-supported. The clast supported portion contains abundant basalt fragments, and one rounded, 0.2 mm particle is isotropic glass with a small gas bubble. The matrix supported portion contains mainly felsic volcanic clasts, including tuff. A partly isotropic, glassy particle with elongated vesicles in the matrix supported portion is petrographically similar to the impact melt particles in the samples above. Apart from the two glassy possible impact melt particles, no shock metamorphic features were found in this sample thin section.	76.02	ICP-OES, NiS-ICP-MS

Table 1. *Continued*. Petrographic descriptions of the El'gygytgyn ICDP drill core samples and impact melt rocks analyzed in this study.

Sample depth (mblf)	Lithology	Microscopic description	Sample mass (g)	Analytical methods
347.3	Upper polymict impact breccia	Unshocked felsic volcanic rock, likely ignimbrite	49.73	ICP-OES
348.1	Upper polymict impact breccia	Unshocked felsic volcanic rock, likely ignimbrite	71.45	ICP-OES
351.8	Upper polymict impact breccia	Unshocked felsic volcanic rock, likely ignimbrite with kaersutite crystals	60.85	ICP-OES
368.7	Upper polymict impact breccia	Unshocked felsic volcanic rock with minor breccia that is mainly composed of felsic volcanic clasts that do not exhibit shock metamorphic overprints	53.61	ICP-OES
381.8	Upper polymict impact breccia	Unshocked ignimbrite clast that is surrounded by a compositionally similar breccia without shock metamorphic features	84.83	ICP-OES
391.6	Mafic inclusion	A brecciated ignimbrite is embedded in a mafic, basaltic melt rock that crystallized small flow-aligned plagioclase laths. No shock metamorphic indicators were found in this thin section	53.19	ICP-OES, NiS-ICP-MS, NiS-ID-ICP-MS
435.4	Upper Ignimbrite	Sample is very similar to that at 517.0 mblf, but it displays an approximately 5 mm thick, unfractured brown melt vein; has elongated, altered melt shards; and contains up to 1.5 mm size kaersutite crystals	54.62	ICP-OES
471.4	Lower polymict impact breccia	Unconsolidated breccia composed of fragments derived from the surrounding ignimbrite and exotic clasts of greenschist, granitoid, and strongly altered mafic rocks. The particulate matrix of this breccia is overgrown with phyllosilicates. No shock indicators were found in the thin section of this sample.	77.57	ICP-OES, NiS-ICP-MS
517.0	Lower Ignimbrite	Pervasively altered, unshocked volcanic rock with matrix of fine phyllosilicates that occasionally exhibits a flow texture. Volcanic melt components are flow textured brown to light brown melt streaks and shard shaped fragments with typical sizes of a few mm. Skeletal to subhedral mineral inclusions of quartz, plagioclase, sanidine, and apatite reach sizes up to several mm. Voids are frequently filled with zeolites and the alteration assemblage also includes carbonate, quartz, chlorite, and cryptocrystalline phyllosilicates.	69.32	ICP-OES
TM8	Glasy impact melt rock	Isotropic, transparent glass that crystallized pyroxene trychite crystals. The glass is layered and contains unmelted clastic debris, including zircon crystals with granular textures likely indicative of incipient thermal decomposition	11.63	ICP-OES, NiS-ICP-MS
TM12	Glasy impact melt rock	Isotropic, transparent glass that crystallized pyroxene trychite crystals. The glass is layered and contains unmelted clastic debris, including quartz crystals with planar deformation features and planar fractures	25.30	ICP-OES, NiS-ICP-MS
TM17	Glasy impact melt rock	Isotropic, transparent glass without liquidus phase crystals. The glass is layered and contains unmelted clastic debris, including quartz crystals with planar deformation features and planar fractures.	16.67	ICP-OES, NiS-ID-ICP-MS

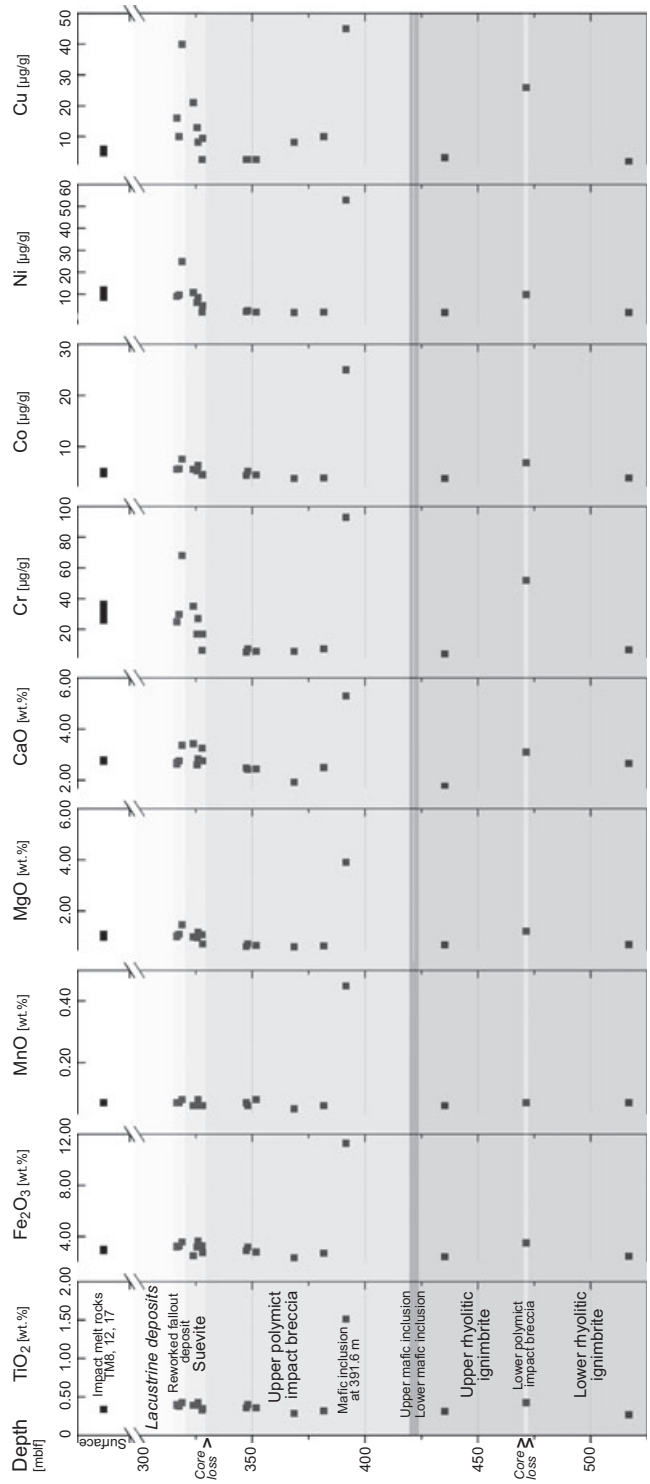

Fig. 2. Profile plot of TiO_2, Fe_2O_3, MnO, MgO, CaO, Cr, Co, Ni, and Cu concentrations versus drill core depth (mblf). The various subunits characterized by Wittmann et al. (2012) are indicated by different shades of gray: lacustrine deposits, reworked fallout deposit, suevite, polymict impact breccia, and rhyolitic ignimbrite. Impact melt rocks, recovered from the surface of the crater, are presented for comparison.

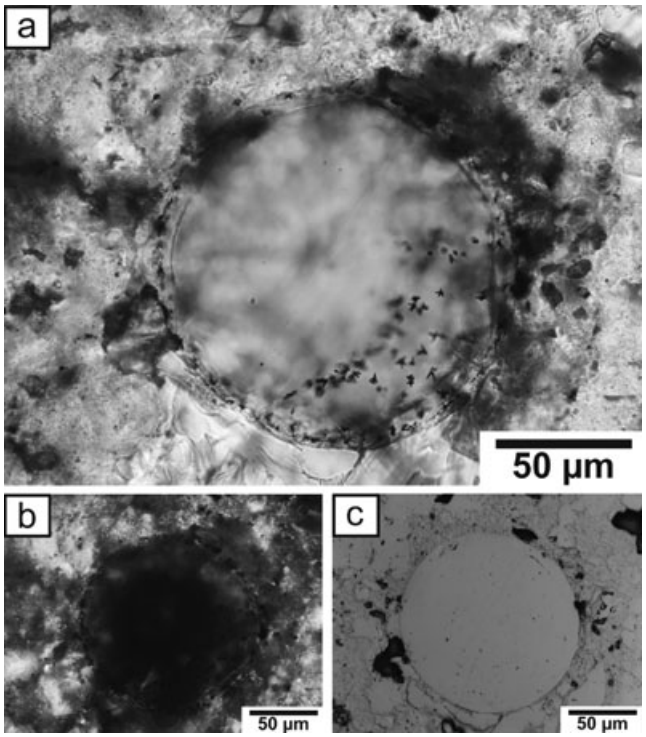

Fig. 3. Micrographs of El'gygtgyn impact spherule Sph8 in a thin section of the reworked fallout deposit at 317.6 mblf. a) Linear polarized light, black crystal inclusions are likely Ni-rich spinels; b) cross-polarized light; c) reflected light. For more details on the spherules recovered from the ICDP drill core and from a terrace deposit of the Enmyvaam River approximately 10 km southeast of the crater center, see Wittmann et al. (2012).

near the western rim of the impact crater were analyzed to complement the study of impact breccia samples from the continuous section of the ICDP drill hole. A short petrographic description of these impact melt rocks is also given in Table 1, with a picture of glassy impact melt clast TM17 in Fig. 1f. More details on these lithologies can be found in Wittmann et al. (2012).

METHODOLOGY

Sample Preparation

All samples were broken into smaller pieces with an agate mortar and pestle, ground to powder with a corundum ball mill, and thoroughly homogenized. The ground drill core sample masses ranged from 14 to 95 g, while the impact melt rock fragments varied in mass from 12 to 25 g (Table 1). These powders were used in all subsequent analyses. Major and trace element abundances were determined using inductively coupled plasma–optical emission spectroscopy

(ICP-OES) at Ghent University (Tables 2 and 3). Based on these results, 10 samples were selected for determination of their PGE contents (Table 4). Because the measured PGE concentrations were only slightly elevated compared with average continental crustal and local target lithology values, five samples were also characterized for their osmium isotopic composition ($^{187}Os/^{188}Os$) at the University of Hawaii (Table 5). This technique is generally considered the most sensitive method for the detection of minute contributions of projectile in terrestrial lithologies, provided no significant ultramafic component occurs in the target (e.g., Koeberl 2007).

Powder aliquots of 3–8 g were dried at 110 °C, and loss on ignition (LOI) was determined by heating at 950 °C for 2 h. After LOI determination, approximately 150 mg of sample powder was homogenized and fused with 0.6 g of 34:66 lithium meta-/tetraborate flux ($LiBO_2/Li_2B_40_7$, Breitländer) in high purity graphite crucibles at 1050 °C. The resulting glass was dissolved in a 2 wt% HNO_3 solution and analyzed with a Spectro Arcos ICP-OES instrument for Na, Mg, Al, Si, P, K, Ca, Ti, Mn, and Fe and selected trace elements (Sc, V, Cr, Co, Ni, Cu, Zn, Sr, Y, Zr, Ba, La, Ce, Nd, Dy, Yb). Selected rock reference materials were dissolved and analyzed following the same procedure, and subsequently used to produce optimal calibration curves, in the range of the sample concentrations measured. Accuracy was monitored by the analysis of secondary international rock standards (United States Geological Survey basalt BCR-2 and Geological Survey of Japan basalt JB-2; Table 3; GeoRem 2012), different from the primary standards used for the calibration curve. Accuracy for trace element determination was additionally verified by comparison with concentrations measured for in-house standards, previously characterized by acid digestion and subsequent analysis via ICP—mass spectrometry (MS). Analysis of drill core samples 318.9, 347.3, and 471.4 mblf, impact melt rock samples TM8 and TM12, and BCR-2, was repeated (Tables 2 and 3). The bias between the experimental results and the corresponding "true values" is estimated to be better than 2% and 10% for major and trace elements above 10 μg g^{-1}, respectively.

The concentrations of the PGEs and Au were determined via a nickel-sulfide (NiS) fire assay sample preparation technique combined with sector field ICP-MS (Thermo-Finnegan Element 2/XR: Ghent University), according to a procedure first described in Plessen and Erzinger (1998), applied in Tagle and Claeys (2005), and further optimized by Goderis et al. (2010). The analytical methodology is described in these studies in detail. The use of large sample masses and external calibration versus a calibration curve for multiple isotopes when possible (^{99}Ru, ^{101}Ru, ^{102}Ru, ^{103}Rh, ^{105}Pd, ^{106}Pd, ^{108}Pd, ^{191}Ir, ^{193}Ir, ^{194}Pt, ^{195}Pt, ^{196}Pt, and ^{197}Au), ensures good analytical accuracy and reproducibility, relatively low limits of detection and quantification (Table 4), and simultaneous measurement of all PGEs (except for Os that volatilizes during the sample preparation procedure). Each solution of approximately 10 ml that was obtained after NiS fire assay preconcentration (aliquot masses are given in Table 4) was characterized twice for its PGE contents via ICP-MS on separate measuring days. The resulting concentrations were averaged and the range of the two analyses was used to estimate the analytical uncertainties for each element according to a method described in Anderson (1987) and Doerffel (1990). The standard deviation of a number (n) of related samples of similar composition is determined as the square root of the square sum of the range of duplicated analyses divided by 2n. The results obtained for international reference materials, diabase TDB-1 with low PGE abundances and the altered peridotite WPR-1 with high PGE concentrations (Canadian Certified Reference Materials Project, CCRMP), are consistent with the certified standard data (Govindaraju 1994) and the recommended values of Meisel and Moser (2004) (Table 4). The latter authors propose to compare new PGE data not only with the original certified values, but also with their compiled literature values until the certified values are up to date. Additionally, the precision and accuracy of the method are regularly tested by analysis of a set of in-house laboratory working standards (large batches of homogenized impact melt rock, K/Pg boundary clay, and meteorites). To determine the procedural limits of detection (instrumental detection limits are significantly lower), procedural PGE blanks were determined by substitution of real samples with SiO_2 powder. Omission of such a PGE-depleted substitute would result in a destruction of the clay crucibles by the aggressive fire assay flux. In this work, limit of detection (LOD) and limit of quantification (LOQ) were calculated as three and ten times the standard deviation (3s and 10s) on 10 reagent blanks, respectively. Experimental values below the LOD are reported as N.D. (not detected), while concentrations below the LOQ are indicated as < numeral value of the LOQ in Table 4.

For the El'gygytgyn samples processed at the University of Hawaii (317.6, 316.7, 391.6 mblf, and TM17; Table 5), Os was preconcentrated from the same bulk rock powders via a NiS fire assay. Each sample powder was accurately weighed (approximately 5 g) and spiked with a tracer solution enriched in

Table 2. Whole rock major and trace element compositions of the El'gygytgyn ICDP drill core impactites determined in this study via ICP-OES.

Sample depth (mblf)	316.7	317.6	318.9	323.9	325.7	326.1	327.8	328.1 (1)	328.1 (2)	328.1 (Avg.)	347.3 (1)	347.3 (2)	347.3 (Avg.)	348.1	351.8	368.7	381.8	391.6	435.4	471.4 (1)	471.4 (2)	471.4 (Avg.)	517.0
SiO_2 (wt%)	69.07	69.58	68.44	67.35	64.26	68.54	67.54	70.30	70.22	70.26	69.57	69.40	69.49	70.85	67.88	71.62	70.79	51.87	67.85	69.61	69.48	69.54	70.43
TiO_2	0.40	0.38	0.43	0.39	0.39	0.43	0.33	0.35	0.35	0.35	0.36	0.36	0.36	0.40	0.36	0.29	0.32	1.51	0.31	0.43	0.43	0.43	0.27
Al_2O_3	16.07	15.64	15.52	17.99	21.73	16.30	17.75	15.70	15.78	15.74	16.58	16.67	16.63	15.23	17.77	15.47	15.55	18.35	18.63	15.67	15.79	15.73	16.20
Fe_2O_3[a]	3.24	3.26	3.60	2.52	3.17	3.64	3.28	2.73	2.74	2.74	2.90	2.92	2.91	3.18	2.80	2.37	2.70	11.27	2.44	3.52	3.49	3.51	2.47
MnO	0.07	0.07	0.08	0.06	0.06	0.08	0.06	0.06	0.06	0.06	0.07	0.07	0.07	0.06	0.08	0.05	0.06	0.45	0.06	0.07	0.07	0.07	0.07
MgO	1.03	1.10	1.47	0.99	0.96	1.18	1.08	0.72	0.73	0.72	0.62	0.62	0.62	0.73	0.66	0.61	0.64	3.90	0.69	1.21	1.20	1.21	0.70
CaO	2.69	2.76	3.37	3.42	2.60	2.84	3.26	2.76	2.78	2.77	2.47	2.49	2.48	2.43	2.44	1.94	2.50	5.30	1.77	3.11	3.08	3.10	2.66
Na_2O	3.25	3.26	3.07	3.37	2.96	3.16	3.24	3.10	3.08	3.09	3.41	3.45	3.43	2.74	3.70	3.08	3.19	4.24	4.27	2.54	2.58	2.56	3.47
K_2O	4.07	3.86	3.92	3.81	3.78	3.71	3.39	4.19	4.18	4.19	3.91	3.91	3.91	4.28	4.22	4.50	4.16	2.11	3.89	3.71	3.75	3.73	3.65
P_2O_5	0.11	0.10	0.11	0.11	0.09	0.11	0.08	0.09	0.09	0.09	0.10	0.10	0.10	0.10	0.10	0.08	0.09	1.00	0.09	0.13	0.13	0.13	0.07
LOI	3.86	4.12	4.78	6.14	5.12	4.97	7.03	3.97	3.97	3.97	3.31	3.31	3.31	3.48	1.40	2.81	3.30	4.94	1.94	4.31	4.31	4.31	2.98
Total	98.21	99.19	98.79	98.60	98.14	99.97	99.52	98.76	97.91		97.84	97.46		98.62	99.01	98.45	99.06	98.61	99.89	98.23	98.66		98.82
Sc (ppm)	7.9	8.6	10.4	9.0	10.1	9.1	5.6	6.6	6.6	6.6	6.0	5.9	6.0	6.7	6.1	4.8	5.6	24	5.4	8.9	8.8	8.9	4.9
V	41	42	51	43	33	48	31	33	33	33	34	33	33	33	30	26	28	188	26	50	50	50	25
Cr	25	30	68	35	17	27	6.4	17	18	17	6.3	4.5	5.4	7.4	5.9	5.7	7.5	93	4.2	51	52	52	6.8
Co	5.6	5.7	7.6	5.6	5.3	6.4	4.6	4.5	4.5	4.5	4.5	4.4	4.4	5.2	4.5	3.8	3.9	25	3.8	6.9	6.9	6.9	3.9
Ni	9.1	9.8	25	11	6.3	8.5	1.9	4.9	4.8	4.9	2.4	1.8	2.1	2.5	1.9	1.8	1.9	53	1.8	9.6	10	9.9	1.8
Cu	16	10	40	21	13	8.2	2.6	9.4	9.4	9.4	2.5	2.5	2.5	2.5	2.6	8.1	10	45	3.1	26	26	26	1.9
Zn	56	58	61	55	61	59	55	49	47	48	53	54	54	59	48	43	49	142	44	54	54	54	49
Sr	228	220	454	752	228	235	202	459	454	456	260	261	261	295	380	204	150	549	220	352	352	352	473
Y	25	30	25	26	26	25	23	21	21	21	21	22	22	26	22	19	22	36	20	22	22	22	20
Zr	207	192	189	164	177	193	211	172	176	174	184	184	184	219	189	189	189	203	186	176	179	177	174
Ba	811	752	856	1033	650	744	661	1137	1099	1118	790	788	789	773	895	747	925	940	796	834	847	841	754
La	35	36	29	32	30	39	38	31	32	31	35	36	35	43	30	33	37	54	36	33	30	32	36
Ce	71	68	64	62	63	74	72	63	63	63	61	60	60	78	63	68	71	118	63	59	60	60	68
Nd	28	33	32	27	19	32	30	31	27	29	19	24	22	36	24	28	27	91	28	27	26	27	26
Dy	2.5	3.8	3.2	2.5	3.3	3.2	1.9	2.5	1.9	2.2	2.5	1.9	2.2	2.5	2.6	2.5	1.9	8.9	2.5	2.5	1.9	2.2	2.5
Yb	1.9	2.5	2.5	1.9	2.0	1.9	1.9	1.9	1.9	1.9	1.9	1.9	1.9	2.5	1.9	1.9	1.9	3.8	1.9	1.9	1.9	1.9	1.9

[a]All Fe as Fe_2O_3.

w% values of major element oxides are normalized to 100%.

Avg. = average of replicated analysis.

Table 3. Whole rock major and trace element compositions of the El'gygytgyn impact melt rocks determined in this study via ICP-OES, in comparison with international reference rock materials BCR-2 and JB-2.

	TM8	TM8	TM8	TM12	TM17	TM17	TM17	BCR-2	BCR-2	BCR-2	BCR-2 (Lit.)	JB-2	JB-2 (Lit.)
	(1)	(2)	(Avg.)		(1)	(2)	(Avg.)	(1)	(2)	(Avg.)			
SiO_2 (wt%)	68.97	68.84	68.90	69.33	69.33	69.19	69.26	54.26	54.24	54.25	54.10	53.06	53.25
TiO_2	0.34	0.34	0.34	0.34	0.34	0.34	0.34	2.29	2.30	2.29	2.26	1.15	1.19
Al_2O_3	16.69	16.77	16.73	16.41	16.29	16.38	16.34	13.35	13.39	13.37	13.50	14.63	14.64
Fe_2O_3[a]	2.93	2.95	2.94	3.00	2.97	2.98	2.97	13.89	13.92	13.91	13.80	14.22	14.25
MnO	0.07	0.07	0.07	0.07	0.07	0.07	0.07	0.20	0.20	0.20	0.20	0.21	0.22
MgO	1.09	1.10	1.10	1.04	0.98	0.99	0.98	3.54	3.56	3.55	3.59	4.53	4.62
CaO	2.76	2.78	2.77	2.74	2.77	2.79	2.78	7.16	7.05	7.10	7.12	9.69	9.82
Na_2O	2.97	2.97	2.97	2.96	3.06	3.08	3.07	3.13	3.16	3.14	3.16	2.02	2.04
K_2O	4.11	4.11	4.11	4.03	4.10	4.11	4.11	1.83	1.84	1.83	1.79	0.40	0.42
P_2O_5	0.08	0.08	0.08	0.07	0.08	0.08	0.08	0.35	0.35	0.35	0.35	0.10	0.10
LOI	0.48	0.48	0.48	0.09	0.12	0.12	0.12						
Total	98.21	97.91		99.39	98.02	98.09		99.01	99.05		99.87	97.15	100.55
Sc (ppm)	7.3	7.3	7.3	7.6	7.9	7.7	7.8	33	33	33	33	53	54
V	36	36	36	38	36	37	37	409	410	409	416	555	575
Cr	36.3	32.2	34	28	26	26	26	21	18	20	18	28	28
Co	5.1	5.1	5.1	5.2	4.7	4.8	4.8	35	34	35	37	28	38
Ni	12	12	12	11	10	8.5	9.1	12	14	13	18	14	17
Cu	5.9	5.9	5.9	5.2	5.4	4.7	5.1	14	14	14	16	234	225
Zn	34	34	34	28	33	33	33	139	138	139	127	113	108
Sr	243	244	244	256	250	251	251	337	339	338	340	176	178
Y	23	23	23	24	24	24	24	36	36	35.7	37.0	22	25
Zr	220	221	221	195	187	188	188	185	188	186	184	47	51
Ba	774	770	772	830	825	825	825	677	682	680	677	213	222
La	32	34	33	36	35	35	35	27	28	27	25	1.9	2.4
Ce	66	63	64	70	62	65	63	46	47	47	53	9.3	6.8
Nd	12	19	15	29	20	19	20	31	23	27	28	N.D.	7
Dy	N.D.	1.7	1.7	2.6	2.0	2.7	2.4	7.6	6.9	7.3	6.4	4.4	3.7
Yb	1.7	1.7	1.7	2.0	2.0	2.0	2.0	4.4	4.4	4.4	3.5	4.4	2.6

[a]All Fe as Fe_2O_3.
wt% values of major element oxides are normalized to 100%.
Avg. = average of replicated analysis.

^{190}Os before fusion to determine concentrations by isotope dilution mass spectrometry. Osmium isotope ratios were measured using a single-collector sector field ICP-MS instrument (ThermoScientific Element 2), according to a procedure slightly modified from Hassler et al. (2000). In this method, OsO_4 becomes volatile after oxidation and is transferred by an Ar gas stream directly into the plasma ("sparging"). An in-house standard is analyzed after every five to six samples in each run to monitor the external reproducibility of the $^{187}Os/^{188}Os$ measurements. The average $^{187}Os/^{188}Os$ ratio of these measurements is 0.1082 ± 0.0028 (2 S.D.; $n = 20$). Ten procedural fusion blanks were analyzed during the course of this study with an average of 0.30 ± 0.20 pg Os g^{-1} sample and a $^{187}Os/^{188}Os$ ratio of approximately 0.87. The total flux mass fused for each blank was 31.5 g. For every set of five to six Os isotope ratio measurements, Ar gas blanks were measured to monitor potential transfer of Os between analyses. Tabulated uncertainties in $^{187}Os/^{188}Os$ are derived from counting statistics (Table 5). Reported Os concentrations were calculated from measured $^{190}Os/^{188}Os$ ratios and all measured ratios yielded 2 sigma errors less than 2%. However, given the very low Os concentrations in these reported impactites, the main source of uncertainty in the data is more likely to result from the procedural blank correction than from the counting statistics. Accuracy of the PGE concentrations is tested by repeated measurement of CCRMP reference material diabase TDB-1. Count rate for TM17 for ^{187}Os was very low (approximately 200 cps), but as this is the only impact melt rock fragment measured, the $^{187}Os/^{188}Os$ is given nonetheless.

Table 4. Concentrations of PGEs and Au in the impactites of El'gygytgyn, determined via NiS fire assay ICP-MS, in comparison with literature data.

Sample depth (mblf)	Ir (ng g^{-1})	Ru (ng g^{-1})	Pt (ng g^{-1})	Rh (ng g^{-1})	Pd (ng g^{-1})	Au (ng g^{-1})	Aliquot mass
TM12	0.142	0.164	0.358	0.081	0.158	0.587	20.6
TM8	0.203	0.231	0.483	0.092	0.319	N.D.	8.0
318.9 (1)	0.262	0.360	0.745	0.120	0.283	N.D.	43.4
318.9 (2)	0.094	0.263	0.424	0.061	0.332	<0.151	4.2
323.9	<0.041	<0.082	0.234	<0.035	N.D.	N.D.	40.4
325.7	N.D.	<0.082	0.391	0.042	0.162	N.D.	20.0
326.1	N.D.	N.D.	0.177	<0.035	N.D.	N.D.	39.2
327.8	<0.041	<0.082	0.182	0.045	<0.109	N.D.	10.6
328.1	<0.041	<0.082	0.289	0.044	N.D.	N.D.	46.0
391.6 (1)	<0.041	0.136	0.296	0.042	0.187	N.D.	21.3
391.6 (2)	<0.041	<0.082	0.349	0.062	0.151	N.D.	10.0
471.4 (1)	0.046	<0.082	0.298	0.049	<0.109	N.D.	46.8
471.4 (2)	0.106	0.187	0.380	0.073	0.191	N.D.	8.3
EL 669-8 IMR[a]	0.111 (±0.021)	n.a.	n.a.	n.a.	n.a.	0.9	n.d.
EL 669-10 IMR[a]	0.073 (±0.017)	n.a.	n.a.	n.a.	n.a.	0.3	n.d.
EL 689 glass bomb[a]	0.024 (±0.010)	n.a.	n.a.	n.a.	n.a.	0.5	n.d.
TDB-1 (n = 4)	0.103	0.301	5.334	0.523	23.321	5.937	
TDB-1 certified[b]	0.150	0.300	5.8 (±1.1)	0.700	22.4 (±1.4)	6.3 (±1.0)	
TDB-1 recommended[c]	0.075	0.179	5.010	0.471	24.3		
LOD	0.012	0.024	0.016	0.010	0.033	0.045	
LOQ	0.041	0.082	0.055	0.035	0.109	0.151	
Analytical uncertainty	0.012	0.012	0.033	0.010	0.059	0.161	

[a]Gurov and Koeberl (2004).
[b]TDB-1 certified values (Govindaraju 1994).
[c]TDB-1 recommended values (Meisel and Moser 2004).
n.d. = not determined; n.a. = not applicable; LOQ = limit of quantification; LOD = limit of detection; analytical uncertainty: see text for detail.

Table 5. Data for the $^{187}Os/^{188}Os$ isotope ratio and Os abundance in El'gygytgyn impactites.

Sample depth (mblf)	$^{187}Os/^{188}Os$	2σ error	Os (ng g^{-1})	% blank correction[d]
TM17[c]	≈0.2		0.003–0.005	8%
316.7[a]	0.239	0.006	0.011	3%
317.6[a]	0.216	0.004	0.012	3%
318.9[a]	0.148	0.001	0.068	0%
391.6[b]	2.800	0.100	0.002	15%

[a]Reworked fallout deposit sample.
[b]Mafic inclusion.
[c]Impact melt rock.
[d]Indicates the magnitude of the blank correction for the Os isotope ratios.

RESULTS

Composition of the Impactite Section in Drill Core ICDP-El'gygytgyn 1C and Implications for Target Rock Components in Impact Melt

Major and trace element concentrations for the 20 bulk rock samples analyzed via ICP-OES in this study are presented in Tables 2 and 3 and Fig. 2. The results obtained for the drill core samples are in good agreement with published data (Gurov et al. 2005; Raschke et al. 2013) and indicate a moderately homogeneous, subalkaline, rhyodacitic character (with minor excursions to trachydacite; Fig. 4). In particular, the reworked fallout deposit is characterized by a homogeneous geochemistry, while the suevite and polymict impact breccia units show larger compositional variability. In the TAS diagram (Fig. 4), all but one whole rock drill core sample measured in this study plot within the range of whole rock compositions of the upper target rock sequence (Gurov et al. 2005). A mafic inclusion at 391.6 mblf (Fig. 1c) displays a basaltic-trachyandesitic composition and stands out with higher abundances of TiO_2, Fe_2O_3, MnO, MgO, CaO, Sc, V, Cr, Co, Ni, Cu, Zn, etc. (Table 2). This constituent is not described as a major component in the upper target rock sequence (Gurov et al. 2005), but is in agreement with preliminary data that reported basaltic target rock fragments in the drill core (Raschke et al. 2013). On a profile plot versus drill core depth, the concentrations for several major (e.g., TiO_2, Fe_2O_3, MnO, MgO, CaO)

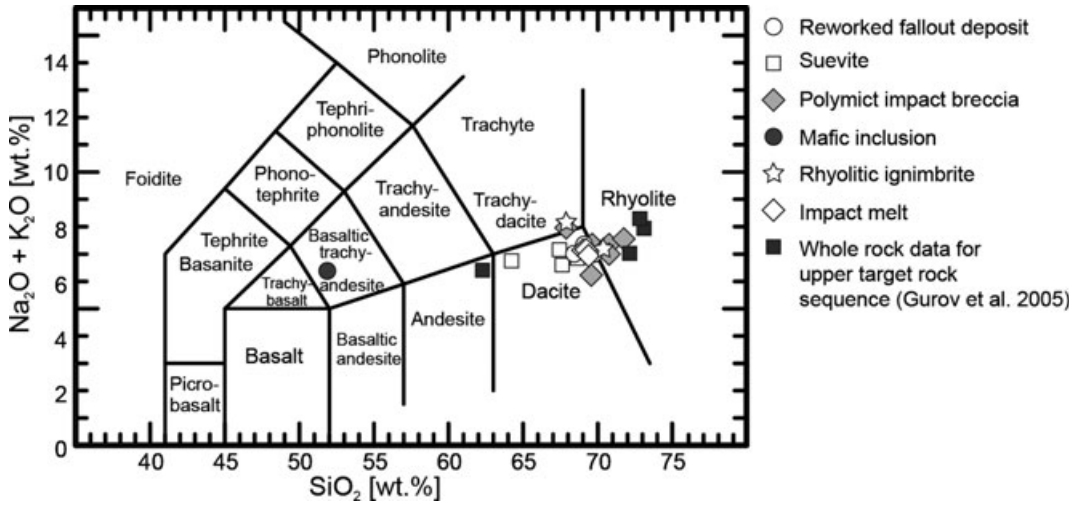

Fig. 4. Total alkali versus silica diagram adapted after Rollinson (1993). Next to the various subunits measured in the study, the whole rock data for the upper target sequence of Gurov et al. (2005) are given. Data are normalized to volatile-free compositions.

and trace (e.g., Cr, Co, Ni, Cu) elements show strong excursions in this mafic inclusion (Fig. 2). Secondary digressions away from the average drill core composition occur at the bottom of the reworked fallout deposit, the top of the suevite interval (318.9–323.9 mblf), and the lower polymict breccia at 471.4 mblf in terms of MgO, CaO, Cr, Co, Ni, and Cu.

Using the rhyolitic ignimbrite encountered in the drill core at 435.4 and 517.0 mblf (upper and lower ignimbrite) as starting material, least squares mixing calculations were performed. The results suggest that an addition of 4.6–13.5 vol% of the mafic inclusions at 391.6 mblf (data from this study) and 391.7, 420.6, 420.9, 422.8, and 423.0 mblf (data for (picro)basaltic inclusions from Raschke et al. 2013), could largely account for the secondary digressions observed for samples 471.4 and 318.9 (χ^2/υ of less than 3; with χ^2 being the sum of least squares, and υ, the number of major and minor elements plus Cr, Co, and Ni, minus the number of components, i.e., rock compositions used for the mixing calculation; Korotev et al. 1995).

Impact-Melt Rock Composition and Comparison with Published Data

The impact melt rock fragments characterized in this study (TM8, 12, 17; Fig. 1f; Table 3) are very homogeneous in terms of major and trace element composition and almost identical in composition to the impact melt rocks (EL669-8 and 10) and glass bombs (EL689, 699, and 985) measured by Gurov and Koeberl (2004). Comparison with the 46 impact melt rocks and impact melt glasses characterized by Gurov et al. (2005) suggests that TM8, 12, and 17 are compositionally most similar to the average for the rhyolitic impact melt rocks from the SW, W, NW, N, NE, and E parts of the crater. Less compositional similarity exists with the andesitic impact melt rocks from the southern part of the crater (Fig. 4). Similar to sample 471.4 mblf, TM8, 12, and 17 can be tentatively modeled to represent mixtures of 2.0 to 6.0 vol% of the basaltic inclusions recovered from drill core intervals between 391.6 and 423.0 mblf (χ^2/υ of less than 3 for major and minor elements, plus Cr, Co, and Ni) with the lower rhyolitic ignimbrite at 517.0 mblf as major hypothetical target (>85 vol%) and minor contributions of the upper rhyolitic ignimbrite at 435.4 mblf.

Moderately Siderophile Element Abundances and Implications for a Meteoritic Component

Strong geochemical variability is observed for the siderophile trace element abundances. The highest siderophile trace element abundances of the 1C drill core bulk rock samples characterized in this study are measured for the mafic inclusion at 391.6 mblf (Cr = 93 μg g^{-1}, Co = 25 μg g^{-1}, Ni = 53 μg g^{-1}), the bottom of the reworked fallout deposits at 318.9 mblf (Cr = 68 μg g^{-1}, Co = 7.6 μg g^{-1}, Ni = 25 μg g^{-1}), and the polymict breccia at 471.4 mblf (Cr = 52 μg g^{-1}, Co = 6.9 μg g^{-1}, Ni = 9.9 μg g^{-1}; Table 2; Fig. 2). Higher concentrations of Cr (up to 945 μg g^{-1}), Co (up to 52 μg g^{-1}), and Ni (up to 278 μg g^{-1}) are reported for basaltic inclusions between 420.6 and 423.0 mblf by Raschke et al. (2013). Gurov et al. (2005) report up to 145 μg g^{-1} Cr, up to 7.9 μg g^{-1} Co, and up to

Table 6. Comparison of the measured Ni/Cr, Ni/Co, and Cr/Co ratios of the El'gygytgyn impactites and impact glass spherules to the upper continental crust and several types of meteorites.

	Ni/Cr	Ni/Co	Cr/Co	Avg. Ni (ppm)[b]	References
UCC	~0.5	1.6–2.6	2.9–5.0		Wedepohl (1995), Taylor and McLennan (1985)
LCC	~0.43	~2.6	~6.0		Wedepohl (1995)
Regression analysis on impactites	0.47 ± 0.04	2.43 ± 0.20	4.16 ± 0.70		This study
Avg. reworked fallout deposit	0.35	2.21	6.20		This study
Avg. suevite	0.30	1.16	3.84		This study
Mafic inclusions	0.19–0.95	2.12–5.84	3.15–21.86		This study, Raschke et al. (2013)
Impact glass spherules	2.37 ± 0.08	16.55 ± 1.51	7.41 ± 1.28	31–1440	Wittmann et al. (2012)
Chondrites					
CI	3.87 ± 0.25	20.87	5.37	10863	Tagle and Berlin (2008)
CM	4.01 ± 0.30	21.27	5.25	12396	Tagle and Berlin (2008)
CO	3.96 ± 0.09	19.73	5.09	13564	Tagle and Berlin (2008)
CV	3.76 ± 0.12	21.26	5.55	13629	Tagle and Berlin (2008)
CK	3.45 ± 0.40	19.34	5.60	12518	Tagle and Berlin (2008)
CR	3.72 ± 0.39	20.71	5.72	13794	Tagle and Berlin (2008)
CH	7.65 ± 0.69	22.86	3.02	25716	Tagle and Berlin (2008)
CB[a]	31.22 ± 7.61	22.27	0.69	66431	Tagle and Berlin (2008)
K	9.72 ± 5.01	21.85	3.28	17172	Tagle and Berlin (2008)
R	3.99 ± 0.19	20.53	5.09	14366	Tagle and Berlin (2008)
H	4.38 ± 0.42	22.07	4.54	16846	Tagle and Berlin (2008)
L	3.22 ± 0.19	22.67	6.40	12936	Tagle and Berlin (2008)
LL	2.64 ± 0.21	21.19	7.78	9585	Tagle and Berlin (2008)
EH	5.79 ± 0.36	21.04	3.59	18006	Tagle and Berlin (2008)
EL	4.77 ± 1.03	20.18	4.33	14676	Tagle and Berlin (2008)
Differentiated achondrites					
Howardite	~0.013	~3.2	~253	65	Tagle (2004)
Eucrites	~0.024	~3.9	~363	103	Tagle (2004)
Diogenites	~0.006	~1.8	~368	36	Tagle (2004)
Angrites	~0.080	~2.9	~43	64	Tagle (2004)
Aubrites	~1.3	~22	~57	1181	Tagle (2004)
Primitive achondrites					
Winonaites	~8.3	~47	~5.7	16300	Tagle (2004)
Acapulcoites	~3.7	~20	~6.1	15799	Tagle (2004)
Lodranites	~4.5	~18	~10	15053	Tagle (2004)
Brachinites	~1.2	~12	~13	2934	Tagle (2004)
Ureilites	0.21–0.24	11–12	49–76	1127	Warren et al. (2006), Tagle (2004)
Iron meteorites	379–4000	12–24	0.003–0.058	6.15–17.1 wt%	Hutchison (2004)

[a]Values for the metallic fraction.
[b]Unless indicated otherwise.

76 μg g^{-1} Ni in "impact glass bomb E-985-101," "porphyritic volcanic rock E-908-73," "glass (fragmental tuff?) E-963-4," and "polymict lithic breccia E-963-14" collected from the crater's surface. However, most impact melt rocks and glass bombs characterized by Gurov and Koeberl (2004), Gurov et al. (2005), and this study contain <50 μg g^{-1} Cr, <7 μg g^{-1} of Co, and up to 21 μg g^{-1} of Ni. These compositions are more or less within the range of typical upper continental crustal (UCC) values (Cr = 35–85 μg g^{-1}, Co = 12–17 μg g^{-1}, Ni = 19–44 μg g^{-1} after Wedepohl [1995] and Taylor and McLennan [1985]) with ratios of e.g., Ni/Cr = 0.19–0.57 and Ni/Co = 0.41–3.3, compared with Ni/Cr = 0.43–0.50 and Ni/Co = 1.6–2.6 for the upper and lower continental crust and Ni/Cr = 2.6–9.7 and Ni/Co = 1923 for chondritic meteorites; Wedepohl 1995; Tagle and Berlin 2008 (Table 6). Nonetheless, the profile plot of the concentrations of various elements versus drill core depth (Fig. 2) indicates that several impactites (e.g., at 318.9, 471.4 mblf and melt rock fragments TM8, 12, 17) are enriched in Cr, Ni, and Cu, whereas most other impactites and target rocks have essentially

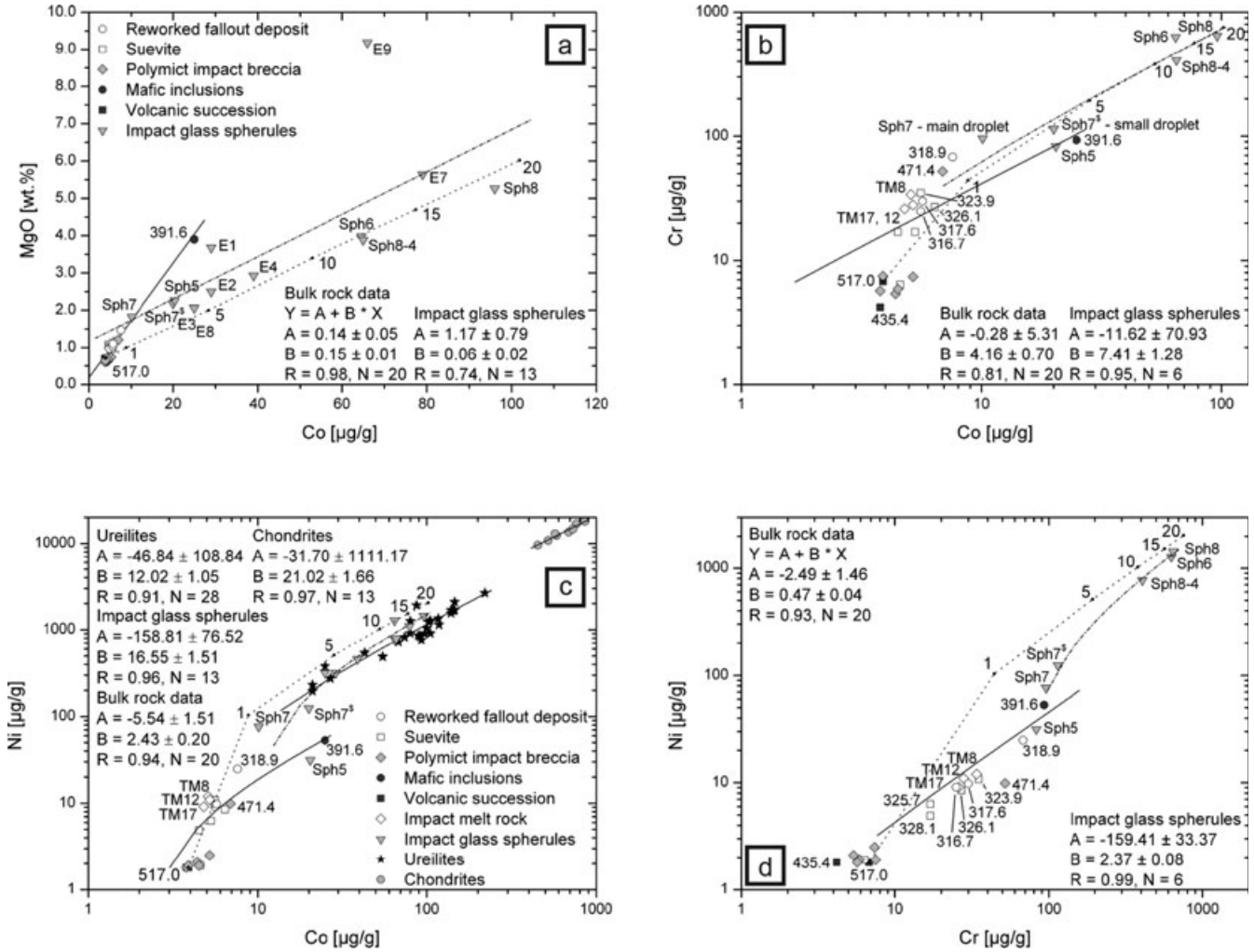

Fig. 5. Plots of (a) MgO versus Co, (b) Cr versus Co, (c) Ni versus Co, and (d) Ni versus Cr. Impact glass spherule data were determined by LA-ICP-MS and EMPA (Wittmann et al. 2012). Characterized impact spherules come from a terrace deposit of the Enmyvaam River approximately 10 km southeast of the crater center and the reworked fallout deposit at 317.6 mblf. Ureilite data from Warren et al. (2006); chondrite data from Tagle and Berlin (2008). Dotted lines mix modeled contributions of 1 to 20 wt% of LL-type ordinary chondrite to the composition of lower rhyolitic ignimbrite at 517.0 mblf. Dash-dot lines reflect linear regression analyses of impact glass spherules, solid lines those calculated for the bulk rock data, ureilites, and chondrites.

the same Co abundance. These observations are in line with those of Va'lter et al. (1982), Gurov and Koeberl (2004), and Gurov et al. (2005), and can at least in part be explained by least squares mixing calculations that add 2.0–13.5 vol% of mafic inclusions to a rhyolitic ignimbrite target.

While the excellent correlation between MgO and Co for the drill core impactites (correlation coefficient R of 0.98; Fig. 5a) indicates an essentially indigenous origin of Co, the source of Cr and Ni is less evident (correlation coefficients R with MgO < 0.50). When plotting the concentrations of Cr and Ni versus Co (Figs. 5b and 5c), a dichotomous distribution for the composition of the samples becomes apparent, separating the mafic inclusions from all other drill core samples. The mafic inclusion at 391.6 mblf, but also the basaltic inclusions at 391.7, 420.6, 420.9, 422.8, and 423.0 mblf (Raschke et al. 2013) display much higher Co concentrations than the reworked fallout deposit, suevite, and impact melt rocks characterized in this study or the Cr-enriched impact glass bomb E-985-101, porphyritic volcanic rockE-908-73, glass E-963-4, and polymict lithic breccia E-963-14 of Gurov et al. (2005). This indicates that the mafic inclusions and similar lithologies are not the only contributors to the moderately siderophile element budget of the drill core impactites. Mixing calculations that use substantial amounts of porphyritic volcanic rock E-908-73 or glass E-963-4 also fail to reproduce the major and trace element abundances of the enriched impactites.

Va'lter et al. (1982) suggested a common source for the impactite Ni and Cr based on the high correlation coefficient (0.80) of the abundances of these two elements as obtained on 40 analyses. These authors concluded that the element enhancement ratios found for the El'gygytgyn impactites compared with the target lithologies resemble most closely the ratios observed in the Novyi Urei meteorite (Ni/Co = 2.4–4, Ni/Cr = 0.25–0.5), suggesting the presence of a ureilitic component in the range of approximately 1 vol%. On a plot of Ni versus Cr (Fig. 5d), the data obtained in this study correlate well, showing a Ni/Cr ratio of 0.47 ± 0.04 ($R = 0.93$, $N = 20$) based on the slope of the linear regression line (close to the Ni/Cr enhancement ratio of 0.54 ± 0.2 of Va'lter et al. 1982). This could be indicative for two-component mixing.

Adolph and Deutsch (2009, 2010) and Wittmann et al. (2012) report chemical data obtained by electron microprobe (EMPA) analysis and laser ablation (LA)—ICP-MS on 7 impact glass spherules and spherule fragments recovered from terrace deposits of the Enmyvaam River outside the crater rim, approximately 10 km southeast of the crater center, and on five spherules from the reworked fallout deposit at 317.6 mblf (Fig. 3). Arguments for the impact origin of the spherules collected outside the crater are presented in Wittmann et al. (2012) and can be summarized as: (1) these spherules are composed of pristine glass, while the target rock clasts in the ICDP drill core indicate pervasive alteration that predates the impact; (2) four of these spherules incorporate accreted lithic debris; (3) the geochemical compositions of these spherules range from rhyolitic to basaltic-andesitic, in large part similar to those of the spherules in samples 316.7 and 317.6 mblf. Because volcanic spherules exclusively form from low-viscosity basaltic melts ($SiO_2 < 52$ wt%) and tend to be homogeneous (Heiken et al. 1974), a volcanic origin for the spherules at El'gygytgyn is implausible.

Several of the studied spherules also appear to contain Ni-rich spinel and an admixed ultramafic component (Wittmann et al. 2012); Fig. 4 plots the MgO, Cr, Co, and Ni data for these glass spherules. Although the spherules are compositionally variable from andesitic to rhyolitic, all but one (Sph5 with Cr = 83 μg g^{-1}, Co = 20 μg g^{-1}, Ni = 31 μg g^{-1}) are characterized by high to very high Cr, Co, and Ni concentrations (Cr up to 646 μg g^{-1}, Co up to 96 μg g^{-1}, Ni up to 1440 μg g^{-1}) and consistently high Ni/Cr of 0.80–2.2, Ni/Co of 6.2–20, and Cr/Co of 5.7–9.8. On the MgO versus Co diagram, 5 of the 13 reported impact spherules are characterized by much higher Co to MgO ratios than measured for the drill core samples (including those of Raschke et al. 2013), plotting away from the MgO/Co correlation line determined for the whole rock impactite concentrations and suggesting an unsampled or uncharacterized contributing source (Fig. 5a). On a plot of Ni versus Co, the correlation coefficient determined for the linear regression line between these 13 samples is excellent (0.96), with a Ni/Co ratio (represented by the slope of the regression line) of 16.55 ± 1.51 (Fig 4c). For the five glass spherules of the reworked fallout deposit at 317.6 mblf (Wittmann et al. 2012), additionally characterized for their Cr content, excellent correlations between Cr, Co, and Ni are also observed ($R > 0.95$; Figs. 5b and 5d). These concentrations and ratios (summarized in Table 6) cannot be derived from upper or lower continental crustal values (Cr = 35–228 μg g^{-1}, Co = 12–38 μg g^{-1}, Ni = 19–99 μg g^{-1}; Wedepohl 1995) or even a component geochemically close to Earth's mantle (Cr = 2520 μg g^{-1}, Co = 102 μg g^{-1}, Ni = 1860 μg g^{-1}, with MgO = 36.8 wt%; Palme and O'Neill 2004), unless strongly fractionated. The Ni/Cr and Cr/Co ratios determined by linear regression for the impact spherules are within the compositional ranges of certain chondrites and primitive achondrites (Table 6). The determined Ni/Co for the impact spherules is intermediate between the ratios determined for ureilites (12.02 ± 1.05, $R = 0.91$ for 28 data points by Warren et al. 2006) and brachinites (approximately 12) and those of chondrites (21.02 ± 1.66, $R = 0.97$ for 13 chondrite types averaged in Tagle and Berlin 2008), lodranites, and acapulcoites (approximately 19–20; Table 6).

Platinum Group Element Abundances

The 12 PGE and Au abundances determined in this study by NiS-ICP-MS are low (over 50% of the measured Ir concentrations fall below the limit of quantification) to slightly elevated compared with average UCC values – Ir = 0.02 ng g^{-1}, Ru = 0.21 ng g^{-1}, Pt = 0.51 ng g^{-1}, Rh = 0.06 ng g^{-1}, Pd = 0.52 ng g^{-1}, and Au = 2.5 ng g^{-1} (Rh and Au from Wedepohl 1995; other PGEs from Peucker-Ehrenbrink and Jahn 2001; Table 4). Iridium contents for these impactites vary from 0.046 to 0.262 ng g^{-1} (Table 4), in the same order of magnitude as the range measured by Gurov and Koeberl (2004) for two impact melt rocks (EL 669-8 and 10) and a glass bomb (EL 689) (Ir = 0.024 ± 0.010 to 0.111 ± 0.021 ng g^{-1}). While the enrichment is more obvious for Ir, Ru, Pt, and Rh, the values for Pd and Au do not appear equally elevated. This observation could be linked to the higher relative mobility of Au and Pd compared with the other PGEs (e.g., Evans et al. 1993), or it could be an inherent characteristic of the PGE enrichment. While correlation

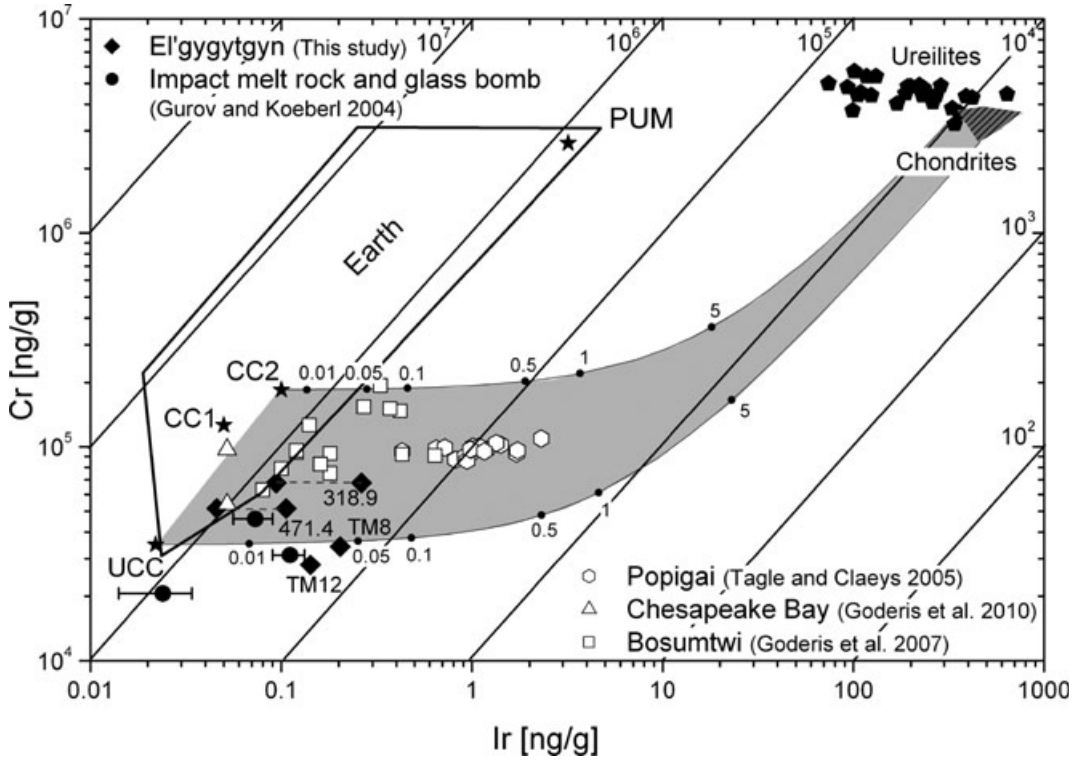

Fig. 6. Double logarithmic plot of the Cr versus Ir concentration of the El'gygytgyn impactites compared with the Cr/Ir ratio in various terrestrial lithologies, chondrites, and ureilites (adapted after Tagle and Hecht 2006; ureilite data from Warren et al. 2006). Values measured at the Bosumtwi, Chesapeake Bay, and Popigai impact structure are presented for comparison (Tagle and Claeys 2005; Goderis et al. 2007, 2010). The gray field indicates the most likely mixing trajectory between chondritic projectiles and common terrestrial targets. Next to the data measured in this study, also data for impact melt rocks and a glass bomb of Gurov and Koeberl (2004) are plotted. UCC = upper continental crust; CC = continental crust; CC1 = Wedepohl (1995); CC2 = Taylor and McLennan (1985); PUM = primitive upper mantle (McDonough and Sun 1995).

coefficients between Ir, Ru, Pt, and Rh vary from good to excellent (R between 0.67 and 0.99), they correlate substantially less with Pd and Au (R between 0.26 and 0.70) and with Cr, Co, and Ni (R = 0.02–0.47). However, the correlations between Cr, Co, and Ni are excellent (R between 0.82–0.94). In several impact-crater studies, strong correlations between moderately and highly siderophile elements have been used to suggest a common origin and to exclude mafic or ultramafic contributions, as well as significant postimpact fractionation or remobilization (e.g., Palme 1980; Morgan and Wandless 1983). At El'gygytgyn, the situation appears more complex because based on least squares mixing calculations, the mafic inclusions could have contributed 2.0–13.5 vol% to the reworked fallout deposit at 318.9 mblf, the polymict impact breccia at 471.4 mblf, and the three impact melt rock fragments.

The reworked fallout deposit at 318.9 mblf (Fig. 1e) shows the highest Cr and Ni values, and has the highest Ir, Ru, Pt, and Rh values for one replicate analysis (but not Co, Pd, and Au; Table 4). Elevated PGE concentrations compared with the average continental crust and the local target background signal (with mafic inclusion 391.6 as the most mafic possible contributor in this study) are also measured for impact melt rocks TM8 and 12 (0.142–0.203 ng g^{-1} Ir) and the lower polymict impact breccia at 471.4 mblf (0.046–0.106 ng g^{-1} Ir; Fig. 1a), concurrent to the anomalous moderately siderophile element (Cr, Co, and Ni) concentrations. The sole exception is the mafic inclusion at 391.6 mblf, where the moderately siderophile element enrichment is not accompanied by significantly elevated PGE abundances. The reported variability for different sample aliquots suggests a heterogeneous distribution of the PGE carrier in the El'gygytgyn impactites. As reported in previous studies (e.g., Hall and Pelchat 1994; Tagle and Claeys 2005), processing larger sample volumes (>10 g) can compensate for these nugget effects, suggesting that the larger sample aliquot analyses are more likely to be representative for the respective drill core intervals.

On a double-logarithmic plot of Cr versus Ir (Fig. 6), the PGE-enriched impactites follow mixing lines that are typical for an admixture of chondritic projectile material (calculated based on average CI carbonaceous chondrites; Tagle and Berlin 2008) to

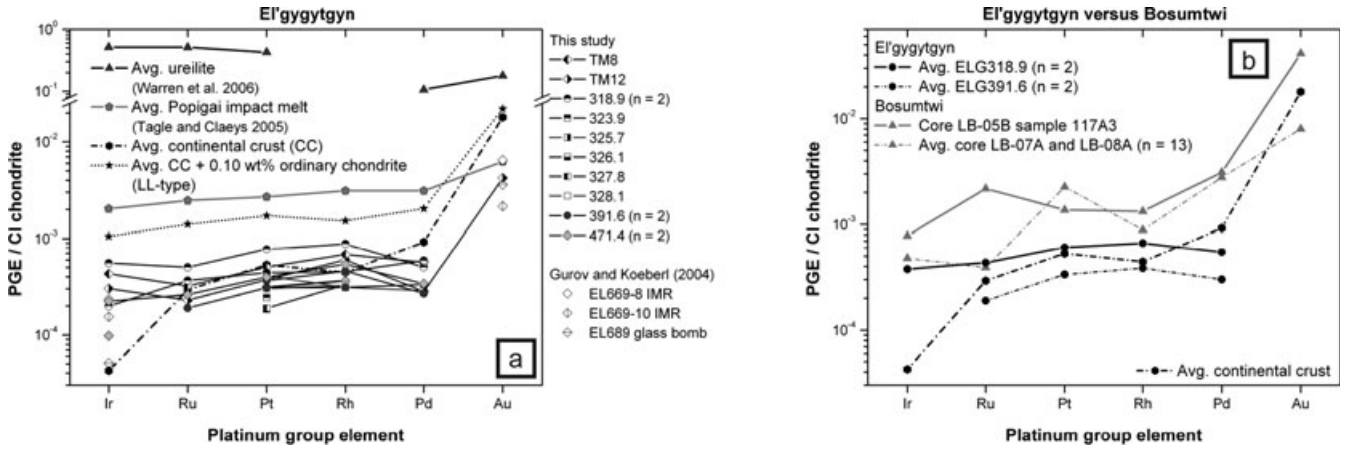

Fig. 7. CI-normalized logarithmic plot of the PGE and Au concentrations of a) the El'gygytgyn ICDP drill core samples and melt rock fragments characterized in this study, in comparison with the average continental crust, the impact melt rocks and glass bomb measured for Ir and Au by Gurov and Koeberl (2004), the average Popigai impact melt (Tagle and Claeys 2005), 0.10 wt% of LL-type ordinary chondrite added to the average continental crust, and the average of ureilites (Warren et al. 2006); b) the ICDP drill core samples from the reworked fallout deposit 318.9 mblf and the mafic inclusion 391.6 mblf of El'gygytgyn in comparison with the averaged LB-07A and LB-08A ICDP drill cores and uppermost impact fallback layer LB-05117A3 of Bosumtwi (Goderis et al. 2007). Values for the continental crust are from Peucker-Ehrenbrink and Jahn (2001); Rh and Au values come from Wedepohl (1995); chondrite values are from Tagle and Berlin (2008). The PGEs are plotted from left to right in order of decreasing condensation temperature.

terrestrial crustal rocks. For comparison, data for impactites from the Bosumtwi, Chesapeake Bay, and Popigai impact structures are also shown (data from Tagle and Claeys 2005; Goderis et al. 2007, 2010). The Popigai impactites contain approximately 0.2 wt% of an ordinary chondritic component (Tagle and Claeys 2005) and plot along a path that tracks the admixture of chondritic material into the continental crust. In contrast, the ICDP-Eyreville drill core samples of the Chesapeake Bay impact crater do not record a distinct meteoritic component (Goderis et al. 2010) and fall within the terrestrial ("Earth") field. In the case of Bosumtwi, where a mafic target rock component with varying Cr and Ir contributions obscures the meteoritic component, up to 0.1 wt% of extraterrestrial material appears dissolved in the suevites of the ICPD cores (Goderis et al. 2007). The El'gygytgyn impactites measured in Gurov and Koeberl (2004) and in this study display only minor PGE enrichment and have a background composition close to upper continental crust (UCC) values (reflected by EL689 glass bomb of Gurov and Koeberl 2004). For a more detailed description of the data used for terrestrial rocks in this plot, see the compilation of literature data in Tagle and Hecht (2006). On a CI carbonaceous chondrite-normalized logarithmic scale, with the PGEs and Au plotted according to decreasing condensation temperatures, all measured El'gygytgyn impactites show comparable, relatively nonfractionated (i.e., flat) chondritic patterns, although similarities to the average continental crust are also evident (Fig. 7).

Osmium Isotope Ratios

To investigate the nature of the PGE enrichment, Os isotope ratios were measured in three reworked fallout deposit samples (316.7, 317.6, and 318.9 mblf), the mafic inclusion at 391.6 mblf, and an impact melt rock fragment (TM17). The presence of a mantle component, such as an ultramafic rock, can apparently be ruled out for most of these El'gygytgyn impactites based on major and trace element abundances (all $Fe_2O_3 \leq 3.6$ wt% and all MgO ≤ 1.5 wt%), with exception of the mafic inclusion at 391.6 mblf. These $^{187}Os/^{188}Os$ ratios can be interpreted as approximate to the initial ratios because the age of the El'gygytgyn impact crater is very young (3.6 Ma; Layer 2000); moreover, the $^{187}Re/^{188}Os$ ratios were not measured in this study. Although the measured Os concentrations are low (≤ 0.068 ng g^{-1}), all reworked fallout deposit samples and the melt rock have much lower $^{187}Os/^{188}Os$ ratios (0.148–0.239) than the mafic inclusion at 391.6 m ($^{187}Os/^{188}Os$ of 2.8). Considering that this inclusion likely has a Paleocene origin and contains low Os abundances, high Re/Os values are likely. In agreement with the siderophile abundance results, the bottom of the reworked fallout deposit at 318.9 mblf displays the highest PGE anomaly (68 pg g^{-1} Os) and lowest $^{187}Os/^{186}Os$ ratio (0.148 $\pm$ 0.001; Table 5). The strongly

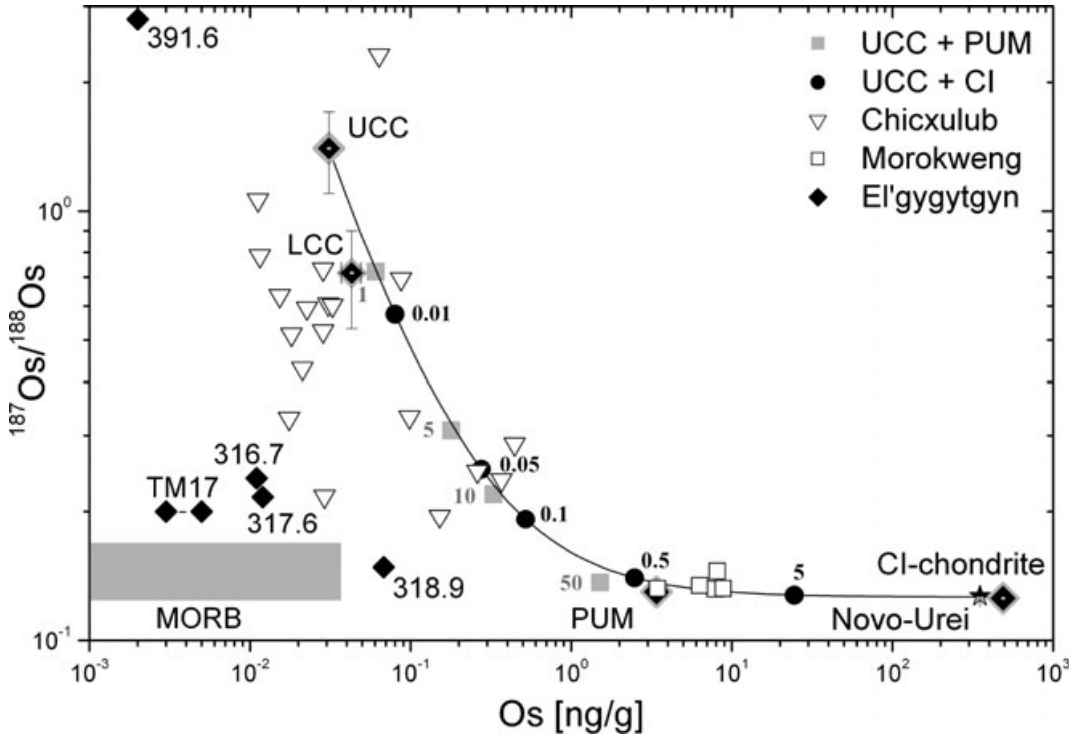

Fig. 8. $^{187}Os/^{188}Os$ isotope ratios versus Os concentrations (ng g^{-1}) for various terrestrial rocks, CI carbonaceous chondrites (Wasson and Kallemeyn 1988), averaged ureilites (Warren et al. 2006; Rankenburg et al. 2007), and impactites of the Morokweng (Koeberl et al. 2002), Chicxulub (Gelinas et al. 2004), and El'gygytgyn impact structures. The curve represents the calculated mixing line between CI chondrite values and the upper continental crust (UCC) (Os = 0.031 ng g^{-1} and $^{187}Os/^{188}Os$ = 1.4; Peucker-Ehrenbrink and Jahn 2001). Percentages of projectile material mixed into hypothetical impact melt are shown as a line with black dots (0.01 to 5 wt%). The mixing trajectory between UCC and primitive upper mantle (PUM) (Os = 3 ng g^{-1} and $^{187}Os/^{188}Os$ = 0.125; McDonough and Sun 1995; Meisel et al. 2001) is indicated by solid squares (1 to 50 wt%) only. Adapted after Tagle and Hecht (2006).

differing Os isotope ratios measured for (1) impact melt rock fragments and reworked fallout deposits, and (2) the basaltic inclusions also characterized by low Os concentrations, indicate the presence of an additional component—with low Os isotope ratios and a relatively flat CI-normalized, logarithmic PGE signature.

Figure 7 plots $^{187}Os/^{188}Os$ isotope ratios versus Os concentrations for various terrestrial rocks (including upper [UCC] and lower [LCC] continental crust and primitive upper mantle [PUM]), CI chondrites (Wasson and Kallemeyn 1988), and the Morokweng (Koeberl et al. 2002), Chicxulub (Gelinas et al. 2004), and El'gygytgyn impactites (this study). While the impactites of the Morokweng structure lie close to a mixing line between a hypothetical CI chondritic impactor and the UCC, the Chicxulub and El'gygytgyn impactites show much lower Os concentrations and higher $^{187}Os/^{188}Os$ ratios. With an average continental crustal target lithology composition—and no apparent contribution from mantle material or young, mantle-derived mafic rocks—the high Os and low $^{187}Os/^{188}Os$ ratios of the Morokweng impactites can be attributed to an extraterrestrial component (Koeberl et al. 2002). For Chicxulub, the samples reflect a mixing trend between the continental crust and a meteoritic component (Gelinas et al. 2004). While most samples have values not substantially different from those of the continental crust (Fig. 8), the ones with higher Os and lower $^{187}Os/^{188}Os$ ratios most likely reflect the presence of an extraterrestrial component below 0.1 wt%, rather than the admixture of 10 wt% mafic rock (Gelinas et al. 2004). For El'gygytgyn, the difference in Os isotopic composition between the mafic contributor(s) and the enriched impactites reflects the presence of uncharacterized or unsampled target rock lithologies and/or a meteoritic component.

DISCUSSION

Meteoritic Component at El'gygytgyn: Diluted, but Distinct?

The amount of meteorite contribution needed to detect, and eventually identify the projectile in an

impactite depends on several parameters: (1) the proportion of siderophile elements in the projectile; (2) the proportion of PGEs in the target lithologies; (3) the homogeneity of the projectile material distribution; and (4) the analytical method applied to identify the extraterrestrial component (e.g., Palme 1980; Tagle and Hecht 2006; Koeberl 2007; Goderis et al. 2012).

Projectiles enriched in highly siderophile elements, i.e., chondrites, stony-iron, and iron meteorites, are more likely to induce a strong enrichment (e.g., more than 0.1 wt% of bulk meteoritic contribution) in impactites that is discernable from background target lithology siderophile element contents. Whereas chondrites are accompanied by elevated Cr abundances of 2575–3810 μg g^{-1} and Ni/Cr ratios that vary between roughly 2 and 7 (Tagle and Berlin 2008), iron meteorites contain approximately two orders of magnitude less Cr (Buchwald 1975). Consequently, iron meteorites display much higher Ni/Cr or lower Cr/Co ratios (up to three orders of magnitude), although exceptions occur (e.g., silicate-rich nonmagmatic iron meteorites; Tagle et al. 2009; Goderis et al. 2009; Table 6).

The situation is less transparent for PGE-poor impactors, such as differentiated achondrites howardites–eucrites–diogenites, aubrites, and angrites. In the absence of clear Ni, Co, and PGE enrichments that are accompanied by elevated Cr values (and low Ni/Cr and high Cr/Co ratios) in impactites, (differentiated) achondritic impactors have been suggested (Koeberl 2007) (Table 6). However, it is often difficult to completely rule out an indigenous (ultra)mafic origin for elevated Cr concentrations. Terrestrial impact structures with little or no enrichment in siderophile elements include Nördlinger Ries, Mistastin, West Clearwater, Saint Martin, Chesapeake Bay, and Manicouagan (Morgan et al. 1975, 1979; Palme et al. 1978, 1981a; Palme 1982; Schmidt and Pernicka 1994; Goderis et al. 2010). For most of these craters, the precise type of impactor has not been constrained so far. Although not all types of projectiles are well characterized or even known (e.g., comets)—meteorite collections sample a subset of the existing cosmic material (e.g., Jenniskens et al. 2009)—some of these structures have tentatively been linked to the impact of achondritic projectiles. The only impact structures where strong cases for achondrite impactors have been presented are Lake Nicholson and Strangways that were likely produced by olivine-rich achondrites, judging from the nature of the PGE enrichments (Wolf et al. 1980; Morgan and Wandless 1983).

In homogenous and continuous impact-melt sheets, where the highest projectile contributions generally occur, it is possible to detect, and eventually characterize, minute ($\leq$0.10 wt%) proportions of a chondritic projectile, sometimes even in the case of a PGE-enriched target (Tagle and Hecht 2006). However, these approaches are not always applicable to less homogenized impactites, as for example, the impact breccias from Bosumtwi, in which target rock contributions mask the meteoritic component (Goderis et al. 2007).

A meteoritic component appears to be present in several El'gygytgyn impactites. Based on the major and trace element abundances, a major contribution (>15 vol%) from a mafic target component (known from regional outcrops and fragments in the drill core) is inadequate to explain all features observed for the analyzed El'gygytgyn impactites. This suggests that these impactites were mainly derived from the upper 620 m thick volcanic succession of rhyolite, dacites, and andesites (cf. Wittmann et al. 2012). Unfortunately, these target lithologies were not characterized for their PGE contents in this study. Nonetheless, the presence of an extraterrestrial component in the El'gygytgyn impactites is confirmed based on (1) the moderately siderophile trace element abundances and nonterrestrial ratios measured for the recovered impact glass spherules and spherule fragments (Wittmann et al. 2012) (Figs. 2 and 4), (2) the double-logarithmic plot of Cr versus Ir concentrations (Fig. 6), (3) the CI-normalized PGE and Au signature (Fig. 7a), and (4) the Os isotopic signature (Fig. 8). An additional, and perhaps even less ambivalent, argument is presented by the nonterrestrial Cr isotopic composition of an impact glass sample from El'gygytgyn that Foriel et al. (2013) determined.

In terms of whole rock analyses, a bulk meteoritic component of up to 0.05 wt% (of hypothetical bulk CI carbonaceous chondrite) can be deduced from the double logarithmic plot of the Cr versus Ir concentration (Fig. 6), with a starting point that is close to the upper continental crust of Wedepohl (1995), for the highest projectile contributions, measured in impact melt rock fragment TM8 and reworked fallout deposit 318.9. As can be observed on this plot, the proportions of meteoritic component (nominal CI chondrite) in the impactites of El'gygytgyn are higher than the values reported for the ICDP-Eyreville drill core of the Chesapeake Bay impact structure. The amount of meteoritic component in El'gygytgyn impactites appears comparable to those of the Chicxulub impactites, but lower than those of the Bosumtwi ICDP drill core (approximately 0.1 wt%) and Popigai impact melt (approximately 0.2 wt%) (Figs. 6, 7, and 8 and references therein). The very diluted meteoritic signature at El'gygytgyn is likely only discernible owing to the relatively low background PGE concentrations in the target lithologies. When comparing the CI-normalized PGE and Au pattern of El'gygytgyn to, for instance, that

of the Popigai impact melt (Fig. 7a) (Tagle and Claeys 2005), the average PGE signature in the El'gygytgyn impactites appears to share characteristics of both the impacted meteorite and the target lithologies.

In terms of the Re-Os isotopic system, the background signal measured for the mafic inclusion 391.6 (with large blank correction) plots more closely to upper continental crustal values. However, the reworked fallout deposit samples and the impact melt rock fragment probably reflect the presence of a diluted meteoritic component. Model mixing calculations indicate the absence of strong target rock contributions to the Os budget and the presence of 0.05–0.10 wt% of bulk CI carbonaceous chondrite material in reworked fallout deposit sample 318.9 (Fig. 8), comparable to the amount of cosmic contribution deduced from the Cr-Ir plot (Fig. 6). Although the Os isotope ratio method is highly sensitive for the detection of a projectile component, it is currently not possible to obtain any specific information about the projectile type with this method.

Distribution of Projectile Material

In order of increasing projectile contribution, this study detected a meteoritic component in (1) the lower polymict lithic breccia, (2) two impact melt fragments, and (3) at the bottom of the fallout deposit. The latter is associated with impact glass spherules, some with Ni-rich spinel and possibly strongly enriched in a meteoritic component based on their moderately siderophile element contents and ratios (Wittmann et al. 2012). As expected, the impact melt rocks—suggested to have the highest probability to contain a meteoritic component (Va'lter et al. 1982)—contain fairly reproducible abundances of Cr, Co, Ni, and Ir (on the order of 100–200 ng g^{-1}; Table 4). Less evident is the slight increase in moderately siderophile and PGE abundances determined for the lower polymict impact breccia. This breccia may consist of debris that was picked up during the radial transport over 2–6 km from near the upper wall of the transient cavity to the current location on top or on the flank of the collapsed central uplift (Wittmann et al. 2012).

Sample 318.9, located in close proximity to the boundary between suevite and reworked fallout deposits at 319.4 mblf, has the highest abundance of impact spherules of approximately 1.4 cm^{-2} among the three samples from the reworked fallout deposit (Wittmann et al. 2012), and it contains the strongest impactor signature. In these respects, it is reminiscent of Bosumtwi's uppermost impact fallback layer, a 30 cm-thick, size-sorted unit that caps the impactite deposits and contains microtektite-like spherules, accretionary lapilli and shocked quartz in its uppermost 10 cm (Koeberl et al. 2007). The observed PGE pattern for this fallback layer is flatter and more similar to that expected for a chondritic contamination compared with the Bosumtwi samples, which are dominated by mafic to ultramafic target rock components (Goderis et al. 2007) (Fig. 7b). It appears that some of the impact glass spherules at El'gygytgyn record a relatively large contribution of meteoritic material based on their MgO, Cr, Co, and Ni abundances and ratios (Wittmann et al. 2012) (Fig. 4). In several impact structures, including the Nördlinger Ries (Pernicka et al. 1987) and Rochechouart (S. Goderis, unpublished data), graded deposits overlying suevites contain a meteoritic component. However, spherules were only found in such deposits at Bosumtwi and El'gygytgyn (Koeberl et al. 2007; Wittmann et al. 2012).

Possible Types of Projectile

A prominent Cr and less pronounced Ni and Ir enrichment combined with the observed siderophile interelement ratios (e.g., Ni/Cr, Cr/Ir, etc.), led several authors to suggest a ureilitic achondrite as possible impactor for El'gygytgyn (e.g., Va'lter et al. 1982; Gurov and Koeberl 2004). The moderately siderophile element contents, Os isotope ratios, and nonfractionated CI-normalized PGE pattern with possible slight depletion in Pd and Au measured for several whole rock impactites of the ICDP–El'gygytgyn lake 1C drill core could be interpreted to record an ureilite impactor. Moreover, the Cr isotopic composition of an impact glass sample is inconsistent with known carbonaceous chondrites, but is within analytical error of eucrites and ordinary chondrites, and nearly identical to the reported values for ureilites (Foriel et al. 2013).

However, provided elemental fractionation (e.g., during volatilization and/or oxidation) and a strongly heterogeneous impactor are precluded, the moderately siderophile element contents and their ratios in the characterized impact glass spherules and spherule fragments, recovered from the reworked fallout deposits and terrace deposits of the Enmyvaam River outside the crater rim, are not characteristic of ureilites. After exclusion of most types of differentiated achondrites (HED, angrites, and aubrites) and iron meteorites based on the Ni/Cr, Ni/Co, and Cr/Co ratios and their generally fractionated CI-normalized PGE patterns, ordinary chondrites remain as the most likely types of projectiles, followed by several types of primitive achondrites (Table 6).

Least squares mixing calculations (Korotev et al. 1995) were used to model the major and minor element compositions plus Cr, Co, and Ni concentrations of

four impact spherules (normalized to 100 wt% with standard deviations recalculated to relative%, which were used as weighting factors) recovered from the reworked fallout deposits at 317.6 mblf. Whole rock compositions of rhyolitic ignimbrite samples 517.0 and 435.4 mblf, mafic inclusion 391.6 mblf, and average compositions of ordinary chondrites (Hutchison 2004) were used as additional mixing components in the models. Successful mixing calculations are presented in Table 7. These results indicate that the composition of the impact glass spherules Sph5, 6, 7, and 8 can be represented by a dominant portion of rhyolitic ignimbrite target rocks (>80%) and 0.50–18 wt% of admixed ordinary chondrite, most likely type-LL. Ignimbrite sample 517.0 mblf was found to be the only required target rock component for all successful mixing calculations. For Sph6, effective mixing results were obtained with additions of 1.0–8.0 wt% of upper ignimbrite sample 435.4 mblf. However, this target rock component is not necessary to produce a successful mixture between lower ignimbrite sample 517.0 and approximately 13 wt% ordinary chondrite. Consistently, mixtures with the LL-chondrite average composition yielded the best melt mixing results, as expressed by the smallest reduced sum of residual squares (χ^2/υ; with χ^2 being the sum of least squares, and υ the number of major, minor, and trace elements minus the number of components, i.e., rock compositions used for the mixing calculation) compared with mixtures with L- and H-chondrite, Lodran, or Acapulco (Tables A1 and 7). It is also noteworthy that the mixing results for Sph6 and Sph8 (χ^2/υ of 2.6 and 1.6) are far more reliable than those for Sph5 (χ^2/υ of 5.6) and (the main part of droplet aggregate-spherule) Sph7 (χ^2/υ of 7.5). At the same time, contributions of 0.05 wt% of LL-type chondritic material led to a significant systematic improvement of the whole rock mixing calculations for the reworked fallout deposit at 318.9 mblf and the melt rock fragments (χ^2/υ below 1). Figure 4 models contributions of 1–20 wt% of LL-type ordinary chondrite to the composition of the lower rhyolitic ignimbrite at 517.0 mblf. On the MgO versus Co plot (Fig. 5a), the modeled contributions follow a line with a slope almost identical to the result of linear regression analysis for the characterized impact glass spherules and spherule fragments (slope $B = 0.06 \pm 0.02$, $R = 0.74$, $N = 13$). On a diagram of Ni versus Cr (Fig. 5d), the dash-dot line resulting from linear regression slightly plots away from the modeled mixing line, suggesting larger relative contributions from lithologies such as the basaltic inclusions between 420 and 423 mblf (Raschke et al. 2013) in spherules Sph5 and Sph7. On this diagram, it also becomes apparent that, while most polymict impact breccias (with exception of 471.4) plot close to the lower rhyolitic ignimbrite at 517.0 mblf, most reworked fallout deposits and suevites, and several impact melt rocks show compositions characteristic for the admixture of minor amounts of basaltic inclusions and/or ordinary chondrite. Similarly, on a plot of Ni versus Co (Fig. 5c), the slightly subchondritic Ni/Co ratio of 16.55 ± 1.51 ($R = 0.96$, $N = 13$) could reflect shallowing of the linear regression slope through the composition of Sph5 and Sph7, due to the larger relative contributions from basaltic inclusions. Additional support for an ordinary chondrite (possibly type-LL) is provided by the Ni/Cr ratio determined by linear regression for the glass spherules of reworked fallout deposit at 317.6 mblf (2.37 ± 0.08; Fig. 9) and the whole rock nonfractionated, chondritic CI-normalized PGE patterns of the reworked fallout deposit at 318.9 mblf and melt rock fragments (Fig. 7).

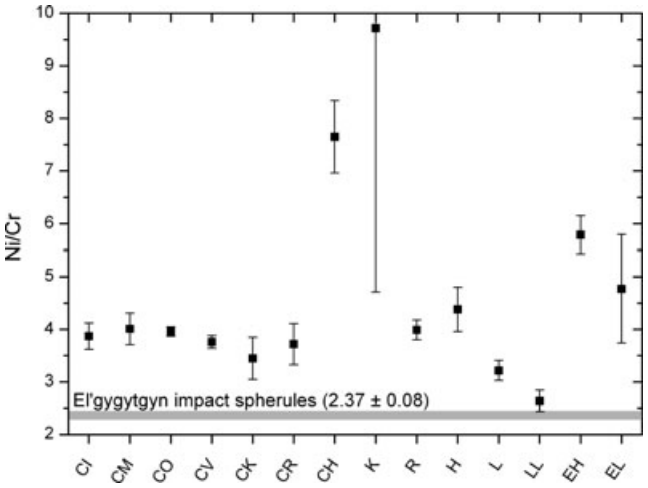

Fig. 9. Plot showing the mean Ni/Cr ratios of various types of chondrites (CI, CM, CO, CV, CK, CR, CH, K, R, H, L, LL, EH, EL) with associated error bars (data from Tagle and Berlin 2008). The Ni/Cr ratio calculated for the El'gygytgyn impact glass spherules ($N = 6$) by linear regression analysis (indicated by light gray bar) is only consistent with LL-type ordinary chondrites.

Implications for the Formation of El'gygytgyn's Microtektite-Like Spherules

Simple mass-balance considerations suggest that the spherules did not form due to fractional condensation from a vapor cloud: given the relatively high abundances of components in the spherules with low volatilization temperatures, such as Na and K, and the constraints for the possible projectile types, it seems most plausible that the El'gygytgyn spherules formed as the result of the accretion of melt droplets of target and ordinary chondritic impactor (compare Wittmann et al. 2012). Subsequently, Ni-rich spinel formed on the

Table 7. Results of least squares melt-mixing calculations.

Sample	LL-chondrite[a] (%)	Lower ignimbrite 517.0 mblf (%)	SiO_2 (wt%)	TiO_2 (wt%)	Al_2O_3 (wt%)	FeO (wt%)	MnO (wt%)	MgO (wt%)	CaO (wt%)	Na_2O [wt%]	K_2O (wt%)	Cr (ppm)	Co (ppm)	Ni (ppm)	Sum oxides (wt%)	Sum χ^2 (–)	χ^2/υ (–)
Sph5	0.5 ± 0.4	94.9 ± 2.4															
		Observed	69.32	0.39	15.16	3.30	0.08	2.25	2.65	2.94	3.90	83	31	20	100.0		
		Estimated	67.08	0.41	15.39	2.25	0.07	0.81	2.54	3.30	3.47	27	58	6	95.4 ± 2.5		
		Difference	−2.23	0.02	0.23	−1.05	−0.01	−1.45	−0.12	0.36	−0.43	−56	27	−14			
		χ^2	3.64	0.98	0.62	5.23	0.15	10.37	0.21	15.71	9.64	7	2	0		55.7	5.6
Sph6	13.1 ± 1.6	86.6 ± 2.6															
		Observed	64.99	0.4	13.79	5.58	0.11	4.14	2.89	3.94	4.12	629	65	1277	100.0		
		Estimated	66.54	0.39	14.32	5.25	0.11	4.15	2.55	3.13	3.17	504	69	1359	99.8 ± 3.1		
		Difference	1.55	−0.01	0.53	−0.33	0.00	0.01	−0.34	−0.81	−0.95	−125	4	82			
		χ^2	0.89	0.18	1.98	0.18	0.01	0.02	0.50	14.28	6.60	2	1	0		27.1	2.6
Sph7-main droplet	1.1 ± 0.5	94.1 ± 2.0															
		Observed	70.13	0.32	14.74	2.8	0.08	1.82	2.45	3.24	4.35	96	10	76	99.9		
		Estimated	67.33	0.41	15.41	2.40	0.07	0.96	2.55	3.31	3.47	48	9	116	95.1 ± 2.1		
		Difference	−2.80	0.09	0.67	−0.40	−0.01	−0.86	0.10	0.07	−0.88	−48	−1	40			
		χ^2	12.63	0.89	12.81	1.03	0.13	6.82	0.04	0.09	32.64	5	3	0		74.6	7.5
Sph8	18.3 ± 0.8	81.6 ± 1.0															
		Observed	65.03	0.36	13.40	6.46	0.10	5.33	3.08	2.87	3.35	646	96	1440	100		
		Estimated	65.10	0.37	13.65	6.29	0.12	5.33	2.51	3.01	3.00	707	95	1916	99.8 ± 1.3		
		Difference	0.07	0.01	0.25	−0.17	0.02	0.00	−0.57	0.14	−0.35	61	−1	476			
		χ^2	0.01	0.01	0.69	0.62	0.49	0.00	5.14	0.88	4.84	0	0	3		15.7	1.6

[a]Average composition of LL-chondrites after Hutchison (2004); χ^2 is the sum of least squares, and υ the number of major, minor, and trace elements minus the number of components, i.e., rock compositions used for the mixing calculation (Korotev et al. 1995). Standard deviations of spherule analyses (Wittmann et al. 2012), recalculated as relative standard deviations in % were used as weighting factors for the mixing calculations. Mixing attempts with target rock compositions of basaltic inclusions and ignimbrite (Table 2; Raschke et al. 2013) can reproduce some of the spherule compositions; however, we found best fits for these calculations with χ^2/υ of 6.1 for Sph5, 20.4 for Sph6, 10.3 for Sph7, and 33.7 for Sph8 that are generally inferior to best fits with LL-chondrite. Mixing calculations using L-chondrite (Hutchison 2004) have consistently higher χ^2 than LL-chondrite and mixtures with H-chondrite (Hutchison 2004), Acapulcoite (using the composition of the Acapulco meteorite [Palme et al. 1981b] as a representative for this primitive achondrite clan), and Lodranite (using the composition of the Lodran meteorite [Fukuoka et al. 1978] as a representative for this primitive achondrite clan) typically yield even higher χ^2/υ and, thus, inferior fits (Table A1).

surface of melt droplets (Fig. 3) during their residence in the ejecta plume/fireball, sometimes prior to droplet accretion. In contrast, condensation from a vaporized achondrite projectile, such as the ureilite suggested in previous studies, would require the preferential incorporation of Ni and Co into the spherules, with close to 100% of the average concentration of these elements in ureilites (Warren et al. 2006) (Fig. 5c), while only approximately 10% of the Cr from an ureilite projectile would have contributed to the spherule composition. This mass-balance consideration seems implausible.

Melt-mixing calculations (Table 7) show that spherule compositions in the ICPD-drill cores can be produced from mixing ignimbrite target rock with LL-chondrite impactor. In contrast, spherules collected SE of the crater rim probably record the presence of an additional, surficial mafic target lithology (Stone et al. 2009; Wittmann et al. 2012). Wittmann et al. (2012) consider the ignimbrite sample 517.0 mblf as representative of surficial target lithologies that are grossly similar to the upper 250–450 m of "ignimbrites" and "tuffs and rhyolitic lava" that constituted the uppermost pre–impact target rock sequence in the SW, W, NW, N, and NE regions of the crater (Gurov and Gurova 1991). Thus, the El'gygytgyn spherules appear to record lateral target rock variations to a depth of <0.5 km. Following scaling relationships of Schmidt and Housen (1987) and constraints from numerical modeling (Collins et al. 2008), a projectile diameter of approximately 1.5 km can be assumed for the El'gygytgyn impact. These constraints can approximate the depth of target lithologies (d_T) that contribute to microtektite-like spherules such as those from El'gygytgyn, to the diameter of a typical asteroidal projectile for the respective crater linked to these spherules (D_P):

$$d_T < D_P/3 \quad (1)$$

Although very tentative, this scaling relationship could be tested and refined by analyzing microtektite-like, glassy spherules from other terrestrial impact craters such as Bosumtwi (Koeberl et al. 2007) and Chicxulub (Sigurdsson et al. 1991).

Ordinary Chondritic Impactors

Chondrites are believed to dominate the main fraction of the extraterrestrial material reaching Earth, not only as meteorites (approximately 85% of the meteorites falling on Earth; Meteoritical Bulletin Database 2012), but possibly also as the impact crater-forming projectiles of structures larger than 2 km (e.g., McDonald et al. 2001; Tagle and Claeys 2005), although the projectile composition down to the specific type of meteorite has been determined for only a small fraction of the confirmed impact structures (approximately 10 of 183 recognized on Earth today, i.e., close to 6% of the current impact crater population; Koeberl 2007; Tagle and Hecht 2006; Goderis et al. 2012).

The fall statistics of meteorites are dominated by ordinary chondrites: 38% L-type, 34.1% H-type, and 7.9% LL-type chondrites (Burbine et al. 2002). Impact structures that resulted from the collisions of ordinary chondritic bodies with Earth include Carancas (0.014 km Ø, type H4-5), New Quebec (3.4 km Ø, type L?), Brent (3.8 km Ø, type L or LL), Wanapitei (7.5 km Ø, type L or LL), Bosumtwi (10.5 km Ø, type H, L, or LL), Lappajärvi (23 km Ø, type H), East Clearwater (26 km Ø, type LL or H?), Morokweng (70 km Ø, type LL), and Popigai (100 km Ø, type L) (Koeberl 2007; Kenkmann et al. 2009; Goderis et al. [2012] and references therein). These classifications are generally based on siderophile element abundances or ratios as well as Os and Cr isotope systematics. However, at Morokweng, a drill core within the impact melt rocks revealed a large (25 cm), unaltered, LL6-chondrite fragment as well as several smaller fragments, while at Carancas, multiple H4-5 chondrite fragments were recovered (Maier et al. 2006; Kenkmann et al. 2009; Weisberg et al. 2009).

Additionally, several Neoarchean-Paleoproterozoic spherule layers from South Africa and Western Australia are interpreted to originate from the impact of ordinary chondrites, on the basis of independent Cr isotope and PGE abundance evidence (e.g., Simonson et al. 2009). Only the Chicxulub impact structure concurrent with the Cretaceous-Paleogene boundary has convincingly been linked to a carbonaceous chondritic projectile (type CM2; Kyte 1998; Shukolyukov and Lugmair 1998; Trinquier et al. 2006). In addition, the 3.5–3.2 Ga old Barberton spherule layers in South Africa have been linked to carbonaceous chondrites (possibly type CV; Kyte et al. 2003).

Class C asteroids appear to be similar to carbonaceous chondritic meteorites (e.g., Zolensky 2005). Ordinary chondrites have recently been convincingly linked to S-type asteroids, the most abundant asteroids in the inner asteroid belt (e.g., Binzel et al. 2004; Abe et al. 2006; Nakamura et al. 2011). The Hayabusa mission returned samples from S (IV)-type asteroid 25143 Itokawa that have been identified as ordinary chondritic (LL4–LL6) (e.g., Nakamura et al. 2011; Yurimoto et al. 2011). These data contradict the assertion of the domination of asteroid populations by C-class asteroids (75% of the asteroids visible from Earth; Bell et al. 1989; Gaffey

et al. 1993), while S-type asteroids only form the second largest group. Nevertheless, the current interpretations of the asteroidal spectra suggest that OC asteroids (S- and Q-type) dominate near-Earth objects (e.g., Pieters and McFadden 1994; Binzel et al. 2004).

Cosmic-ray exposure ages of LL-type ordinary chondrites record a major peak at approximately 15 Ma, consistent with a collisional breakup event, and minor clusters at approximately 10 Ma, 28 Ma, and 40–50 Ma (Marti and Graf 1992). However, the systematics of ^{40}Ar-^{39}Ar retention ages show that only minor heating occurred during the roughly 15 Ma collision of the LL-chondrite parent body. The youngest ^{40}Ar-^{39}Ar degassing episode recorded in an LL chondrite meteorite so far occurred approximately 400 Ma ago (e.g., Bogard 2011; Swindle et al. 2011).

CONCLUSIONS

This study tests the hypothesis for an ureilite impactor at the El'gygytgyn impact structure and concludes that an ordinary chondritic projectile is more likely.

1. Least squares mixing calculations using the small suite of samples analyzed in this study indicate that the (upper) polymict impact breccias in the El'gygytgyn 1C drill core are dominated by a rhyolitic ignimbrite composition, with only a minor addition of a basaltic (mafic) component (up to 13.5 wt%). The bulk rock composition of El'gygytgyn-ICDP 1C drill core samples and melt rock fragments recovered from the western rim of the impact crater appear to be derived from the upper 0.6 km of the target rock sequence. This is similar to the observations made for the impact melt particles in the suevite unit of this drill core (Wittmann et al. 2012). As the sampled mafic inclusions are not exposed at the surface, pronounced Cr and smaller Ni enrichments of characterized impactites led previous studies to suggest the presence of a primitive achondrite (ureilite) meteoritic contribution (Va'lter et al. 1982; Gurov and Koeberl 2004; Gurov et al. 2005).
2. The occurrence of a meteoritic component is confirmed based on: (1) the significantly enriched abundances and nonterrestrial ratios of the moderately siderophile elements measured for recovered impact glass spherules and spherule fragments (Wittmann et al. 2012); (2) a slight Ir enrichment with flat, nonfractionated CI-normalized logarithmic PGE patterns for the reworked fallout deposit and several impact rock fragments; (3) Os isotope ratios that are inconsistent with the target rock composition (including mafic, basaltic inclusion 391.6); and (4) the reported nonterrestrial Cr isotopic composition of an impact glass sample (Foriel et al. 2013). Provided elemental fractionation (e.g., during volatilization and/or oxidation) and a strongly heterogeneous impactor are precluded, the moderately siderophile element contents and their ratios in the characterized impact glass spherules and spherule fragments are not characteristic of ureilites. After exclusion of most types of differentiated achondrites (HED, angrites, and aubrites) and iron meteorites based on the Ni/Cr, Ni/Co, and Cr/Co ratios and their generally fractionated CI-normalized PGE patterns, and carbonaceous chondrites based on the Cr isotope ratios measured for an impact glass (Foriel et al. 2013), ordinary chondrites remain as the most likely types of projectiles, followed by several types of primitive achondrites (Table 6).
3. The compositions of the characterized impact spherules and spherule fragments can be modeled as mixtures between rhyolitic ignimbrite target lithologies and 0.50 to 18 wt% of ordinary chondrite, with LL-type chondrites yielding the best fit (Table 7). Mixing models involving primitive achondritic and (ultra)mafic target contributions cannot produce the relative abundances of Cr, Co, and Ni of the spherules in acceptable approximation.

   The whole rock meteoritic enrichment is highest at the bottom of the reworked spherule-bearing fallout deposit, in impact melt rock fragments, and minor in a polymict impact breccia. Although the exact relationship with the presence of compositionally diverse impact glass spherules is not yet fully understood, the base of the reworked fallout deposit records the finest fraction of ejecta, suggesting that reworking and dilution were less effective there during redeposition. The absence of any PGE-enriched target lithologies is essential for the detection and the identification of the very dilute projectile component at El'gygytgyn (approximately 0.05 wt% of nominal ordinary chondrite, possibly type-LL). This amount is comparable to the range of extraterrestrial components observed at many impact structures and ejecta materials (e.g., Tagle et al. 2004; Tagle and Claeys 2005; Goderis et al. 2007, 2012; Koeberl 2007). Similar to the low abundance of shock features and impact melt (Wittmann et al. 2012), the projectile component is too diluted for detection in the suevite unit.
4. The microtektite-like spherules from El'gygytgyn indicate formation as aggregates of melt droplets sourced from the upper target rock sequences and an ordinary chondritic impactor. Mass-balance

considerations discredit formation due to condensation from an impactor vapor cloud. Tentatively, a scaling relationship is deduced between the depth of target lithologies that contributed to the microtektite-like spherules at El'gygytgyn and the assumed projectile diameter for that impact.

Acknowledgments—S. G. is a postdoctoral fellow of the Research Foundation–Flanders (FWO). P. C. and F. V. acknowledge the support of Research Foundation Flanders (grants G.A078.11 and G.0021.11). We gratefully acknowledge Tim Martin (Greensboro Day School) for the donation of impact melt rock samples TM8-17; Kentaro Tanaka for sample grinding at the VUB; David Kring for support at the LPI, Houston; Ulli Raschke (MfN Berlin) for sample processing and sharing his manuscripts for this proceedings volume; Julien Foriel for sharing his manuscript for this proceedings volume; Roald Tagle for the use of his meteorite siderophile element database; the El'gygytgyn Scientific Party and its sponsors (ICDP, Austrian Federal Ministry of Science and Research, Federal Ministry of Education and Research, Germany, German Science Foundation, Russian Academy of Sciences, U.S. National Science Foundation); Leonie Adolph for her to work on El'gygtgyn impact spherules; Michael Roden (Dept. of Geology, University of Georgia) for allowing to use the microscopy lab at UGA. We thank Fred Moynier, Christian Koeberl, and an anonymous reviewer for their thoughtful comments that helped to improve the manuscript significantly.

Editorial Handling—Dr. Christian Koeberl

REFERENCES

Abe M., Tagaki Y., Kitazato K., Abe S., Hiroi T., Vilas F., Clark B. E., Abell P. A., Lederer S. M., Jarvis K. S., Nimura T., and Fujiwara A. 2006. Near-infrared spectral results of asteroid Itokawa from the Hayabusa spacecraft. *Science* 312:1334–1338.

Adolph L. and Deutsch A. 2009. Glass spherules related to the El'gygtgyn impact crater (Siberia) (abstract #1116). 41st Lunar and Planetary Science Conference. CD-ROM.

Adolph L. and Deutsch A. 2010. Trace element analysis of impact glass spherules of the El'gygytgyn crater, Siberia (abstract #2421). 42nd Lunar and Planetary Science Conference. CD-ROM.

Alvarez L. W., Alvarez W., Asaro F., and Michel H. V. 1980. Extraterrestrial cause for the Cretaceous-Tertiary extinction. *Science* 208:1095–1108.

Anderson R. L. 1987. *Practical statistics for analytical chemists*. New York: Van Nostrand Reinhold. 352 p.

Bell J. F., Davis D. R., Hartmann W. K., and Gaffey M. J. 1989. Asteroids: The big picture. In *Asteroids II*, edited by Binzel R. P., Gehrels T., and Matthews M. S. Tucson, Arizona: The University of Arizona Press. pp. 921–945.

Belyi V. F. 1998. Impactogenesis and volcanism of the El'gygytgyn depression. *Petrologiya* 6:86–99.

Binzel R. P., Rivikin A. S., Stuart S. S., Harris A. W., and Bus S. J. 2004. Observed spectral properties of near-Earth objects: Results for population distribution, source regions, and space weathering processes. *Icarus* 170:259–294.

Bogard D. D. 2011. K-Ar ages of meteorites: Clues to parent-body thermal histories. *Chemie der Erde* 71:207–226.

Buchwald V. F. 1975. *Handbook of iron meteorites*. Berkeley: University of California Press. 1418 p.

Burbine T. H., McCoy T. J., Meibom A., Gladman B., and Keil K. 2002. Meteoritic parent bodies: Their number and identification. In *Asteroids III*, edited by Bottke W. F., Jr., Cellino A., Paolicchi P., and Binzel R. P. Tucson, Arizona: The University of Arizona Press. pp. 653–667.

Claeys P., Kiessling W., and Alvarez W. 2002. Distribution of Chicxulub ejecta at the Cretaceous-Tertiary boundary. In *Catastrophic events and mass extinctions: Impacts and beyond*, edited by Koeberl C. and MacLeod K. G. Boulder, Colorado: Geological Society of America. pp. 55–68.

Collins G. S., Kenkmann T., Osinski G. R., and Wünnemann K. 2008. Mid-sized complex crater formation in mixed crystalline-sedimentary targets: Insight from modeling and observation. *Meteoritics & Planetary Science* 43:1955–1977.

Dabizha A. I. and Feldman V. I. 1982. Geophysical characteristics of some astroblemes of the USSR. *Meteoritika* 40:91–101.

Doerffel K. 1990. *Statistik in der analytischen chemie*. Leipzig: VEB Deutscher Verlag für Grundstoffindustrie GmbH. 256 p.

Earth Impact Database. 2012. Earth Impact Database: http://www.passc.net/EarthImpactDatabase/index.html. Accessed December 15, 2012.

Evans N. J., Gregoire D. C., Grieve R. A. F., Goodfellow W. D., and Veizer J. 1993. Use of platinum-group elements for impactor identification: Terrestrial impact craters and Cretaceous–Tertiary boundary. *Geochimica et Cosmochimica Acta* 57:3737–3748.

Feldman V. I., Granovsky L. B., Kapustina I. G., Karoteeva N. N., Sazonova L. V., and Dabija A. I. 1981. Meteorite crater El'gygytgyn. In *Impactites*, edited by Marakhushev A. A. Moscow: Moscow State University Press. pp. 70–92.

Foriel J., Moynier F., Schulz T., and Koeberl C. 2013. Chromium isotope anomaly in an El'gygytgyn crater impactite: Evidence for a ureilite projectile. *Meteoritics & Planetary Science* 48, doi: 10.1111/maps.12116.

Fukuoka T., Ma M.-S., Wakita H., and Schmitt R. A. 1978. Lodran: The residue of limited partial melting of matter like a hybrid between H and E chondrites (abstract). 9th Lunar and Planetary Science Conference. p. 356.

Gaffey M. J., Burbine T. H., and Binzel R. P. 1993. Asteroid spectroscopy: Progress and perspectives. *Meteoritics & Planetary Science* 28:161–187.

Gebhardt A. C., Niessen F., and Kopsch C. 2006. Central ring structure identified in one of the world's best-preserved impact craters. *Geology* 34:145–148.

Gelinas A., Kring D. A., Zurcher L., Urrutia-Fucugauchi J., Morton O., and Walker R. J. 2004. Osmium isotope constraints on the proportion of bolide component in Chicxulub impact melt rocks. *Meteoritics & Planetary Science* 39:1003–1008.

GeoRem. 2012. http://georem.mpch-mainz.gwdg.de. Accessed December 15, 2012.

Glushkova O. and Smirnov V. 2005. General geology and geography. In *Ber. Polarforsch. Meeresforsch.*, edited by Melles M., Minyuk P., Bringham-Grette J., and Juschus O. Leipzig: Institute for Geophysics and Geology. pp. 14–18.

Goderis S., Tagle R., Schmitt R. T., Erzinger J., and Claeys P. 2007. Platinum group elements provide no indication of a meteoritic component in ICDP cores from the Bosumtwi crater, Ghana. *Meteoritics & Planetary Science* 42:731–741.

Goderis S., Kalleson E., Tagle R., Dypvik H., Schmitt R. T., Erzinger J., and Claeys P. 2009. A non-magmatic iron projectile for the Gardnos impact event. *Chemical Geology* 258:145–156.

Goderis S., Hertogen J., Vanhaecke F., and Claeys P. 2010. Siderophile elements from the Eyreville drill cores of the Chesapeake Bay impact structure do not constrain the nature of the projectile. In *Large meteorite impacts and planetary evolution IV*, edited by Gibson R. L. and Reimold W. U. GSA Special Paper 465. Boulder, Colorado: Geological Society of America. pp. 395–409.

Goderis S., Paquay F., and Claeys P. 2012. Projectile identification in terrestrial impact structures and ejecta material. In *Impact cratering: Processes and products*, edited by Osinski G. and Pierazzo E. New York: Wiley-Blackwell. pp. 223–239.

Govindaraju K. 1994. Compilation of working values and description for 383 geostandards. *Geostandards Newsletter* 18:1–154.

Grieve R. A. F., Dence M. R., and Robertson P. B. 1977. Cratering processes: A interpreted from the occurrence of impact melts. In *Impact and explosion cratering*, edited by Roddy D. J., Pepi R. O., and Merrill R. B. New York: Pergamon Press. pp. 791–814.

Gurov E. P. and Gurova E. P. 1991. *Geological structure and rock composition of impact structures*. Kiev: Naukova Dumka Press. 160 p.

Gurov E. P. and Koeberl C. 2004. Shocked rocks and impact glasses from the El'gygytgyn impact structure. Russia. *Meteoritics & Planetary Science* 39:1495–1508.

Gurov E. P., Valter A. A., Gurova E. P., and Serebrennikov A. I. 1978. Explosion meteorite crater Elgygytgyn, Chukotka. *Doklady Akademiia Nauk SSSR* 240:1407–1410.

Gurov E. P., Valter A. A., Gurova E. P., and Kotlovskaya F. I. 1979a. Elgygytgyn impact crater, Chukotka: Shock metamorphsim of volcanic rocks. Proceedings, 10th Lunar and Planetary Science Conference. pp. 479–481.

Gurov E. P., Gurova E. P., and Rakitskaia R. B. 1979b. Stishovite and coesite in shock-metamorphosed rocks of the El'gygytgyn crater in Chukotka. *Doklady Akademiia Nauk SSSR* 248:213–216.

Gurov E., Koeberl C., Reimold W. U., Brandstätter F., and Amare K. 2005. Shock metamorphism of siliceous volcanic rocks of the El'gygytgyn impact crater (Chukotka, Russia). In *Large meteorite impacts III*, edited by Kenkmann T., Hörz F., and Deutsch A. Boulder, Colorado: Geological Society of America. pp. 391–412.

Gurov E. P., Koeberl C., and Yamnichenko A. 2007. El'gygytgyn impact crater, Russia: Structure, tectonics, and morphology. *Meteoritics & Planetary Science* 42:307–319.

Hall G. E. M. and Pelchat J. C. 1994. Analysis of geochemical materials for gold, platinum and palladium at low ppb levels by fire assay-ICP mass spectrometry. *Chemical Geology* 115:61–72.

Hassler D. R., Peucker-Ehrenbrink B., and Ravizza G. E. 2000. Rapid determination of Os isotopic composition by sparging OsO_4 into a magnetic-sector ICP-MS. *Chemical Geology* 166:1–14.

Heiken G. H., McKay D. S., and Brown R. W. 1974. Lunar deposits of possible pyroclastic origin. *Geochimica et Cosmochimica Acta* 38:1703–1738.

Hutchison R. 2004. *Meteorites. A petrologic, chemical and isotopic synthesis*. Cambridge: Cambridge University Press. 506 p.

Jenniskens P., Shaddad M. H., Numan D., Elsir S., Kudoda A. M., Zolensky M. E., Le L., Robinson G. A., Friedrich J. M., Rumble D., Steele A., Chesley S. R., Fitzsimmons A., Duddy S., Hsieh H. H., Ramsay G., Brown P. G., Edwards W. N., Tagliaferri E., Boslough M. B., Spalding R. E., Dantowitz R., Kozubal M., Pravec P., Borovicka J., Charvat Z., Vaubaillon J., Kuiper J., Albers J., Bishop J. L., Mancinelli R. L., Sandford S. A., Milam S. N., Nuevo M., and Worden S. P. 2009. The impact and recovery of asteroid 2008 TC_3. *Nature* 458:485–488.

Kapustina I. G., Feldman V. I., and Kolesov G. M. 1985. Behaviour of some meteoritic material indicator elements in process of impact melt degassing. Proceedings, 16th Lunar and Planetary Science Conference. pp. 422–423.

Kenkmann T., Artemieva N. A., Wunnemann K., Poelchau M. H., Elbeshausen D., and del Prado H. N. 2009. The Carancas meteorite impact crater, Peru: Geologic surveying and modeling of crater formation and atmospheric passage. *Meteoritics & Planetary Science* 44:985–1000.

Koeberl C. 2007. The geochemistry and cosmochemistry of impacts. In *Meteorites, comets, and planets*, edited by Holland H. D. and Turekian K. K. Treatise on Geochemistry, vol. 1. Elsevier. pp. 1.28.1–1.28.52, doi:10.1016/B978-008043751-4/00228-5, online edition.

Koeberl C., Peucker-Ehrenbrink B., Reimold W. U., Shukolyukov A., and Lugmair G. W. 2002. Comparison of Os and Cr isotopic methods for the detection of meteoritic components in impactites: Examples from the Morokweng and Vredefort impact structures, South Africa. In *Catastrophic events & mass extinctions: Impacts and beyond*, edited by Koeberl C. and MacLeod K. G. Boulder, Colorado: Geological Society of America. pp. 607–617.

Koeberl C., Brandstätter F., Glass B. P., Hecht L., Mader D., and Reimold W. U. 2007. Uppermost impact fallback layer in the Bosumtwi crater (Ghana): Mineralogy, geochemistry, and comparison with Ivory Coast tektites. *Meteoritics & Planetary Science* 42:709–729.

Koeberl C., Pittarello L., Reimold U., Raschke U., Brigham-Grette J., Melles M., and Minyuk P. 2012. El'gygytgyn impact crater, Chukotka, Arctic Russia: Impact cratering aspects of the 2009 ICDP drilling project. *Meteoritics & Planetary Science*. 48, doi:10.1111/maps.12146.

Korotev R. L., Haskin L. A., and Jolliff B. L. 1995. A simulated geochemical rover mission to the Taurus-Littrow valley of the Moon. *Journal of Geophysical Research* 100:14,403–14,420.

Kyte F. T. 1998. A meteorite from the Cretaceous/Tertiary boundary. *Nature* 396:237–239.

Kyte F. T., Shukolyukov A., Lugmair G. W., Lowe D. R., and Byerly G. R. 2003. Early Archean spherule beds:

Chromium isotopes confirm origin through multiple impacts of projectiles of carbonaceous chondrite type. *Geology* 31:283–286.

Layer P. W. 2000. Argon-40/argon-39 age of the El'gygytgyn impact event, Chukotka. Russia. *Meteoritics & Planetary Science* 35:591–600.

Maier W. D., Andreoli M. A. G., McDonald I., Higgins M. D., Boyce A. J., Shukolyukov A., Lugmair G. W., Ashwal L. D., Graser P., Ripley E. M., and Hart R. J. 2006. Discovery of a 25-cm asteroid clast in the giant Morokweng impact crater, South Africa. *Nature* 411:203–206.

Marti K., and Graf T. 1992. Cosmic-ray exposure history of ordinary chondrites. *Annual Review of Earth and Planetary Sciences* 20:221–243.

McDonald I. 2002. Clearwater East impact structure: A re-interpretation of the projectile type using new platinum-group element data. *Meteoritics & Planetary Science* 37:459–464.

McDonald I., Andreoli M. A. G., Hart R. J., and Tredoux M. 2001. Platinum-group elements in the Morokweng impact structure, South Africa: Evidence for the impact of a large ordinary chondrite projectile at the Jurassic-Cretaceous boundary. *Geochimica et Cosmochimica Acta* 65:299–309.

McDonough W. F. and Sun S. S. 1995. The composition of the Earth. *Chemical Geology* 120:223–253.

Meisel T. and Moser J. 2004. Reference materials for geochemical PGE analysis: New analytical data for Ru, Rh, Pd, Os, Ir, Pt and Re by isotope dilution ICP-MS in 11 geological reference materials. *Chemical Geology* 208:319–338.

Meisel T., Walker R. J., Irving A. J., and Lorand J.-P. 2001. Osmium isotopic compositions of mantle xenoliths: A global perspective. *Geochimica et Cosmochimica Acta* 65:1311–1323.

Melles M., Minyuk P., Brigham-Grette J., and Juschus O., eds. 2005. The expedition El'gygytgyn Lake 2003 (Siberian Arctic). *Ber. Polarforsch. Meeresforsch*. Leipzig: Institute for Geophysics and Geology. 139 p.

Melles M., Brigham-Grette J., Minyuk P., Koeberl C., Andreev A., Cook T., Fedorov G., Gebhardt C., Haltia-Hovi E., Kukkonen M., Nowaczyk N., Schwamborn G., Wennrich V., and Party T. E. G. S. 2011. The Lake El'gygytgyn Scientific Drilling Project—Conquering Arctic challenges through continental drilling. *Scientific Drilling* 11:15–40.

Melles M., Brigham-Grette J., Minyuk P. S., Nowaczyk N. R., Wennrich V., DeConto R. M., Anderson P. M., Andreev A. A., Coletti A., Cook T. L., Haltia-Hovi E., Kukkonen M., Lozhkin A. V., Rosén P., Tarasov P., Vogel H., and Wagner B. 2012. 2.8 million years of Arctic climate change from Lake El'gygytgyn, NE Russia. *Science* 337:315–320.

Meteoritical Bulletin Database. 2012. http://www.lpi.usra.edu/meteor/. Accessed December 15, 2012.

Morgan J. W. and Wandless G. A. 1983. Strangways Crater, northern territory, Australia: Siderophile element enrichment and lithophile element fractionation. *Journal of Geophysical Research* 88:A819–A829.

Morgan J. W., Ganapathy R., and Anders E. 1975. Meteoritic material in four terrestrial meteorite craters. Proceedings, 6th Lunar Science Conference. pp. 1609–1623.

Morgan J. W., Janssens M.-J., Hertogen J., Gros J., and Takahashi H. 1979. Ries impact crater, southern Germany: Search for meteoritic material. *Geochimica et Cosmochimica Acta* 43:803–815.

Nakamura T., Noguchi T., Tanaka M., Zolensky M. E., Kimura M., Tsuchiyama A., Nakato A., Ogami T., Ishida H., Uesugi M., Yada T., Shirai K., Fujimura A., Okazaki R., Sandford S. A., Ishibashi Y., Abe M., Okada T., Ueno M., Mukai T., Yoshikawa M., and Kawaguchi J. 2011. Itokawa dust particles: A direct link between S-type asteroids and ordinary chondrites. *Science* 333:1113–1116.

Nowaczyk N. R., Minyuk P., Melles M., Brigham-Grette J., Glushkova O., Nolan M., Lozhkin A. V., Stetsenko T. V., Andersen P. M., and Forman S. L. 2002. Magnetostratigraphic results from impact crater Lake El'gygytgyn, northeastern Siberia: A 300 kyr long high-resolution terrestrial palaeoclimatic record from the Arctic. *Geophysical Journal International* 150:109–126.

Palme H. 1980. The meteoritic contamination of terrestrial and lunar impact melts and the problem of indigenous siderophiles in the lunar highland. Proceedings, 11th Lunar and Planetary Science Conference. pp. 481–506.

Palme H. 1982. Identification of projectiles of large terrestrial impact craters and some implications for the interpretation of Ir-rich Cretaceous/Tertiary boundary layers. In *Geological implication of impacts of large asteroids and comets on Earth*, edited by Silver L. T. and Schultz P. H. Boulder, Colorado: Geological Society of America. pp. 223–233.

Palme H., Janssens M.-J., Takahasi H., Anders E., and Hertogen J. 1978. Meteorite material at five large impact craters. *Geochimica et Cosmochimica Acta* 42:313–323.

Palme H., Grieve R. A. F., and Wolf R. 1981a. Identification of the projectile at the Brent crater and further consideration of projectile types at terrestrial craters. *Geochimica et Cosmochimica Acta* 45:2417–2424.

Palme H., Schultz L., Spettel B., Weber H. W., Wänke H., Michel-Levy M. C., and Lorin J. C. 1981b. The Acapulco meteorite: Chemistry, mineralogy and irradiation effects. *Geochimica et Cosmochimica Acta* 45:727–752.

Palme H. and O'Neill H. St. C. 2004. Cosmochemical estimates of mantle composition. In Mantle and core, *Treatise on Geochemistry*, vol. 2, edited by Holland H. D. and Turrekian K. K. Amsterdam: Elsevier. pp. 1–38.

Pernicka E., Horn P., and Pohl J. 1987. Chemical record of the projectile in the graded fall-back sedimentary unit from the Ries Crater, Germany. *Earth and Planetary Science Letters* 86:113–121.

Peucker-Ehrenbrink B. and Jahn B.-M. 2001. Rhenium–osmium isotope systematics and platinum-group element concentrations: Loess and the upper continental crust. *Geochemistry Geophysics Geosystems* 2, doi:10.1029/2001GC000172.

Pieters C. M. and McFadden L. A. 1994. Meteorite and asteroid reflectance spectroscopy: Clues to early solar system processes. *Annual Review of Earth and Planetary Sciences* 22:457–497.

Plessen H.-G. and Erzinger J. 1998. Determination of the platinum-group elements and gold in twenty rock reference material by inductively coupled plasma-mass spectrometry (ICPMS) after pre-concentration by nickel fire assay. *Geostandards Newsletter* 22:187–194.

Rankenburg K., Brandon A. D., and Humayan M. 2007. Osmium isotope systematics of ureilites. *Geochimica et Cosmochimica Acta* 71:2402–2413.

Raschke U., Reimold W. U., and Schmitt R. T. 2013. Petrography and geochemistry of the impactites of the ICDP drill core D1c from Lake El'gygytgyn, NE Russia. *Meteoritics & Planetary Science* 48, doi:10.1111/maps.12087.

Rollinson H. R. 1993. *Using geochemical data: Evaluation, presentation, interpretation*. Harlow, UK: Longman Publishing Group. 352 p.

Schmidt R. M. and Housen K. R. 1987. Some recent advances in the scaling of impact and explosion cratering. *International Journal of Impact Engineering* 5:543–560.

Schmidt G. and Pernicka E. 1994. The determination of platinum group elements (PGE) in target rocks and fall-back material of the Nördlinger Ries impact crater (Germany). *Geochimica et Cosmochimica Acta* 58:5083–5090.

Shukolyukov A. and Lugmair G. W. 1998. Isotopic evidence for the Cretaceous-Tertiary impactor and its type. *Science* 282:927–929.

Sigurdsson H., D'Hondt S., Arthur M. A., Bralower T. J., Zachos J. C., van Fossen M., and Channell J. E. T. 1991. Glass from the Cretaceous/Tertiary boundary in Haiti. *Nature* 349:482–487.

Simonson B. M., McDonald I., Shukolyukov A., Koeberl C., Reimold U. W., and Lugmair G. W. 2009. Geochemistry of 2.63–2.49 Ga impact spherule layers and implications for stratigraphic correlations and impact processes. *Precambrian Research* 175:51–76.

Smit J. and Hertogen J. 1980. An extraterrestrial event at the Cretaceous-Tertiary boundary. *Nature* 285:198–200.

Stone D. B., Layer P. W., and Raikevich M. I. 2009. Age and paleomagnetism of the Okhotsk-Chukotka Volcanic Belt (OCVB) near Lake El'gygytgyn, Chukotka, Russia. *Stephan Mueller Special Publication Series* 4:243–260.

Swindle T. D., Weirich J. R., Isachsen C. E., Wittmann A., and Kring D. A. 2011. ^{40}Ar-^{39}Ar dating of Larkman nunatak 06299: comparison to paired LAR 06298 and to other LL chondrites (abstract #5497). 74th Annual Meteoritical Society Meeting. CD-ROM.

Tagle R. 2004. Platingruppenelemente in Meteoriten und Gesteinen irdischer Impaktkrater: Identifizierung der Einschlagskörper. Ph.D. thesis. Humboldt-Universität, Berlin, Germany.

Tagle R. and Berlin J. 2008. A database of chondrite analyses including platinum group elements, Ni, Co., Au, and Cr: Implications for the identification of chondritic projectiles. *Meteoritics & Planetary Science* 43:541–559.

Tagle R. and Claeys P. 2005. An ordinary chondrite impactor for the Popigai crater, Siberia. *Geochimica et Cosmochimica Acta* 69:2877–2889.

Tagle R. and Hecht L. 2006. Geochemical identification of projectiles in impact rocks. *Meteoritics & Planetary Science* 41:1721–1735.

Tagle R., Erzinger J., Hecht L., Schmitt R. T., Stoffler D., and Claeys P. 2004. Platinum group elements in impactites of the ICDP Chicxulub drill core Yaxcopoil-1: Are there traces of the projectile? *Meteoritics & Planetary Science* 39:1009–1016.

Tagle R., Schmitt R. T., and Erzinger J. 2009. Identification of the projectile component in the impact structures Rochechouart France and Sääksjärvi, Finland: Implications for the impactor population for the Earth. *Geochimica et Cosmochimica Acta* 73:4891–4906.

Taylor S. R. and McLennan S. M. 1985. *The continental crust: Its composition and evolution*. Oxford: Blackwell Publication. p. 312.

Trinquier A., Birck J.-L., and Allègre C. J. 2006. The nature of the KT impactor. A ^{54}Cr reappraisal. *Earth and Planetary Science Letters* 241:780–788.

Va'lter A. A., Barchuk I. F., Bulkin V. S., Ogorodnik A. F., and Kotishevskaya E. Y. 1982. The El'gygytgyn meteorite: Probable composition. *Soviet Astronomical Letters (Pisma Astr. Zh.)* 8:115–120.

Warren P. H., Ulff-Møller F., Huber H., and Kallemeyn G. W. 2006. Siderophile geochemistry of ureilites: A record of early stages of planetesimal core formation. *Geochimica et Cosmochimica Acta* 70:2104–2126.

Wasson J. T. and Kallemeyn G. W. 1988. Composition of chondrites. *Philosophical Transactions of the Royal Society of London A* 325:535–544.

Wedepohl K. H. 1995. The composition of the continental crust. *Geochimica et Cosmochimica Acta* 59:1217–1232.

Weisberg M. K., Smith C., Benedix G., Folco L., Righter K., Zipfel J., Yamaguchi A., and Chennaoui Aoudjehane H. 2009. The Meteoritical Bulletin, No. 95. *Meteoritics & Planetary Science* 44:1–33.

Wittmann A., Goderis S., Claeys P., Vanhaecke F., Deutsch A., and Adolph L. 2013. Petrology of impactites from the El'gygytgyn crater: Breccias in ICDP-drill hole 1C, glassy impact melt rocks and spherules. *Meteoritics & Planetary Science* 48, doi:10.1111/maps.12019.

Wolf R., Woodrow A. B., and Grieve R. A. F. 1980. Meteoritic material at four Canadian impact craters. *Geochimica et Cosmochimica Acta* 44:1015–1022.

Yurimoto H., Abe K., Abe M., Ebihara M., Fujimura A., Hashiguchi M., Hashizume K., Ireland T. R., Itoh S., Katayama J., Kato C., Kawaguchi J., Kawasaki N., Kitajima F., Kobayashi S., Meike T., Mukai T., Nagao K., Nakamura T., Naraoka H., Noguchi T., Okazaki R., Park C., Sakamoto N., Seto Y., Takei M., Tsuchiyama A., Uesugi M., Wakaki S., Yada T., Yamamoto K., Yoshikawa M., and Zolensky M. E. 2011. Oxygen isotopic composition of asteroidal material returned from Itokawa by the Hayabusa mission. *Science* 333:1116–1119.

Zolensky M. E. 2005. Extraterrestrial water. *Elements* 1:39–44.

APPENDIX

Table A1. Results of least squares mixing calculations of El'gygytgyn spherule Sph8 from drill core sample 317.6 mblf. Mass-balance considerations suggest that the compositions of spherules that exhibit a possible impactor component based on their Cr, Co, and Ni abundances, are unlikely the product of an impact by a differentiated achondrite, because of the flat (i.e., chondritic) CI-normalized PGE signature of several bulk El'gygytgyn impactites as well as the absolute Ni abundance and Ni/Cr, Ni/Co, and Cr/Co ratios determined for the El'gygytgyn spherules (Table 6). Of the primitive achondrite clans, the Ni/Cr, Ni/Co, and Cr/Co ratios of acapulcoites and lodranites are closest to those measured for the El'gygytgyn impact spherules, while ureilites and brachinites appear incompatible with regard to absolute Ni abundances and Ni/Cr ratios. Chromium isotope analyses by Foriel et al. (2013) exclude carbonaceous chondrites as possible impactor types. Of the remaining primitive achondrites, ordinary chondrites, K-, R-, and E-chondrites, LL-type ordinary chondrites match closest to the El'gygytgyn impact spherules in terms of the Ni/Cr and Cr/Co ratios (Table 6). To illustrate the melt-mixing modeling for various possible projectile types and known target rocks, Table A1 shows the results for the best fits to the composition of spherule Sph8 recovered from the fallout deposit in the ICDP drill core at 317.6 mblf. LL-chondrite compositions consistently provided the best fit for the El'gygytgyn spherules with significant Cr, Co, and Ni enrichment

Impactor component[a] (%)	Target components[b] (%)	SiO_2 (wt%)	TiO_2 (wt%)	Al_2O_3 (wt%)	FeO (wt%)	MnO (wt%)	MgO (wt%)	CaO (wt%)	Na_2O (wt%)	K_2O (wt%)	Cr (ppm)	Co (ppm)	Ni (ppm)	Sum oxides (wt%)	Sum χ^2 (–)	χ^2/υ (–)
None	31.8 ± 10.5 Mafic Block & 66.0 ± 10.0 Lower Ignimbrite															
	Observed	65.03	0.36	13.40	6.46	0.10	5.33	3.08	2.87	3.35	646	96	1440	100.0		
	Estimated	62.61	0.68	16.71	6.32	0.11	3.53	2.92	3.17	2.50	149	15	34	98.7 ± 13.7		
	Difference	−2.42	0.32	3.31	−0.14	0.01	−1.80	−0.16	0.30	−0.85	−497	−81	−1406			
	χ^2	16.78	7.07	121.11	0.43	0.20	56.28	0.39	3.90	28.47	13	60	26		334.0	33.4
18.3 ± 0.8%	81.6 ± 1.0 Lower Ignimbrite															
LL-chondrite	Observed	65.03	0.36	13.40	6.46	0.10	5.33	3.08	2.87	3.35	646	96	1440	100.0		
	Estimated	65.10	0.37	13.65	6.29	0.12	5.33	2.51	3.01	3.00	707	95	1916	99.8 ± 1.3		
	Difference	0.07	0.01	0.25	−0.17	0.02	0.00	−0.57	0.14	−0.35	61	−1	476			
	χ^2	0.01	0.01	0.69	0.62	0.49	0.00	5.14	0.88	4.84	0	0	3		15.7	1.6
17.2 ± 0.9%	82.5 ± 1.2 Lower Ignimbrite															
L-chondrite	Observed	65.03	0.36	13.40	6.46	0.10	5.33	3.08	2.87	3.35	646	96	1440	100.0		
	Estimated	64.93	0.37	13.77	6.59	0.11	4.82	2.51	3.03	3.03	672	105	2064	99.6 ± 1.5		
	Difference	−0.10	0.01	0.37	0.13	0.01	−0.51	−0.57	0.16	−0.32	26	9	624			
	χ^2	0.03	0.00	1.48	0.35	0.20	4.44	5.20	1.12	4.10	0	1	5		22.8	2.3
14.6 ± 1.3%	84.5 ± 2.0 Lower Ignimbrite															
H-chondrite	Observed	65.03	0.36	13.40	6.46	0.10	5.33	3.08	2.87	3.35	646	96	1440	100.0		
	Estimated	64.65	0.38	14.00	6.89	0.10	3.88	2.50	3.06	3.10	523	118	2265	99.0 ± 2.4		
	Difference	−0.38	0.01	0.60	0.43	0.00	−1.45	−0.58	0.19	−0.26	−123	22	825			
	χ^2	0.42	0.01	3.93	3.74	0.00	36.70	5.46	1.57	2.54	1	4	9		69.0	6.9
10.3 ± 2.1%	75.4 ± 6.5 Lower Ignimbrite & 13.4 ± 8.1 Mafic Block															
Acapulco	Observed	65.03	0.36	13.40	6.46	0.10	5.33	3.08	2.87	3.35	646	96	1440	100.0		
	Estimated	64.01	0.47	14.85	6.67	0.11	3.89	2.61	3.08	2.90	761	123	2113	99.2 ± 10.6		
	Difference	−1.02	0.11	1.45	0.21	0.01	−1.44	−0.47	0.21	−0.45	115.35	27	673			
	χ^2	2.97	0.93	23.15	0.95	0.17	36.10	3.54	2.02	7.93	1	6	6		90.9	10.1

Table A1. *Continued.* Results of least squares mixing calculations of El'gygytgyn spherule Sph8 from drill core sample 317.6 mblf. Mass-balance considerations suggest that the compositions of spherules that exhibit a possible impactor component based on their Cr, Co, and Ni abundances, are unlikely the product of an impact by a differentiated achondrite, because of the flat (i.e., chondritic) CI-normalized PGE signature of several bulk El'gygytgyn impactites as well as the absolute Ni abundance and Ni/Cr, Ni/Co, and Cr/Co ratios determined for the El'gygytgyn spherules (Table 6). Of the primitive achondrite clans, the Ni/Cr, Ni/Co, and Cr/Co ratios of acapulcoites and lodranites are closest to those measured for the El'gygytgyn impact spherules, while ureilites and brachinites appear incompatible with regard to absolute Ni abundances and Ni/Cr ratios. Chromium isotope analyses by Foriel et al. (2013) exclude carbonaceous chondrites as possible impactor types. Of the remaining primitive achondrites, ordinary chondrites, K-, R-, and E-chondrites, LL-type ordinary chondrites match closest to the El'gygytgyn impact spherules in terms of the Ni/Cr and Cr/Co ratios (Table 6). To illustrate the melt-mixing modeling for various possible projectile types and known target rocks, Table A1 shows the results for the best fits to the composition of spherule Sph8 recovered from the fallout deposit in the ICDP drill core at 317.6 mblf. LL-chondrite compositions consistently provided the best fit for the El'gygytgyn spherules with significant Cr, Co, and Ni enrichment

Impactor component[a] (%)	Target components[b] (%)	SiO_2 (wt%)	TiO_2 (wt%)	Al_2O_3 (wt%)	FeO (wt%)	MnO (wt%)	MgO (wt%)	CaO (wt%)	Na_2O (wt%)	K_2O (wt%)	Cr (ppm)	Co (ppm)	Ni (ppm)	Sum oxides (wt%)	Sum χ^2 (–)	χ^2/υ (–)
9.7 ± 2.2%	78.8 ± 7.5 Lower Ignimbrite & 10.4 ± 9.2 Mafic Block															
Lodran	Observed	65.03	0.36	13.40	6.46	0.10	5.33	3.08	2.87	3.35	646	96	1440	100.0		
	Estimated	64.11	0.46	14.68	6.96	0.10	3.61	2.52	3.04	2.99	398	118	2066	98.9 ± 12.0		
	Difference	−0.92	0.10	1.28	0.50	0.00	−1.72	−0.56	0.17	−0.36	−248	22	626			
	χ^2	2.42	0.72	18.14	5.25	0.02	51.59	4.99	1.25	5.20	3	4	5		102.5	11.4

[a] Average composition of H-, L-, and LL-chondrites after Hutchison (2004), Acapulco after Palme et al. (1981b), and Lodran after Fukuoka et al. (1978).

[b] Target components are "Lower Ignimbrite" sample 517.0 mblf, "Basalt Intrusion" sample 391.6 mblf (cf. Table 2), and "Mafic Block" sample 420.9 mblf of Raschke et al. (2013).

χ^2 is the sum of least squares, and υ the number of major, minor, and trace elements minus the number of components, i.e., rock compositions used for the mixing calculation (Korotev et al. 1995). Standard deviations of analyses of Sph8 ("observed," Wittmann et al. 2012), recalcualted as relative standard deviations in%, were used as weighting factors for the mixing calculations.